

POLITECNICO DI TORINO

Master of Science in Petroleum and Mining Engineering



**THE USE OF MEASURING WHILE DRILLING (MWD) TECHNOLOGY
FOR AUTOMATIC IDENTIFICATION OF DISCONTINUITIES**

Supervisor:

Prof.Engr. Marilena Cardu

Co.Supervisor:

Prof.Engr. Pablo Segarra

Tutor:

Engr. Alberto Fernández

Candidate:

Zahir Elharith Mohammedelamein Ahmed

July-2022

Acknowledgements

First, I would like to say, this whole journey would not have been the same or even possible to go through if I had not met my dear friend, my mentor; Prof. Marilena Cardu. There are no words that can describe how much gratitude and respect I have for you; I am so grateful to have met an amazing, kind, and caring person, like you, thank you very much for everything.

Special and warm thanks to Prof. Pablo Segarra and Dr. Alberto Fernandez for their continuous support, availability, and knowledge that guided me through this work. Thank you for everything I have learned so far from you.

To my family, I am thankful for all the support and love you gave to me throughout this journey; you are all the reason why I strive to achieve more, I am what I am because of all of you. Special thanks to my brothers for always being there whenever I needed them, I am so grateful that you have always been my undoubtful resort in life, you are all my backbone.

Finally yet importantly, and as the saying goes "It's not where you are in life, it's who you have by your side that matters" , to my friends, Thank you for making so many ordinary moments, extraordinary. I am Thankful for always giving me the extra push I need.

Abstract

The demand for a proper optimization in mining operations that operate on drill and blast is increasing, starting from the initial steps such as drilling until further downstream operations, such as processing. The number of possibilities that the digitalization is bringing is enormous, allows among others to record the control parameters of the drill rig, providing a high resolution data set that can be used for a better and more detailed geo-mechanical characterization of the rock mass and consequently to adapt the charging of the explosive to rock conditions.

This work applies a recent methodology developed by the Explosive and Blasting Group of Universidad Politécnica de Madrid (UPM) to detect discontinuities from drilling data. Data measurements for two blasts from 17 blastholes have been analyzed with the aim of validating this approach. To define this model, direct measurements of the rock structure have been obtained with an optical televiewer.

The resulting images of the borehole walls have been analyzed through WellCAD software to assess the geometrical properties such as (orientation and aperture) of discontinuities. Afterwards, a binary vector has been constructed that comprises (ones) for discontinuities and (zeros) for massive rock. The drilling data (five pressures, while penetration rate was not available) have been processed using state of the art techniques to remove spurious effect that may mask the effect of the rock mass. Variations of these data are considered to calculate an index that peaks when a discontinuity is crossed by the hole. Values of this index above a threshold are defined then as ones (or discontinuities), while the rest of the signal is defined as zero (or massive rock). To define the best model, several normalized variability parameters, and thresholds, defined as percentiles from (50 to 95) of the discontinuity index, are tested.

The classification accuracy (or ratio of correct prediction) is used to define the best model. This occurs for the combination of the normalized variability of the percussive and air pressure with weights of 20 and 80%, respectively and threshold percentile of 95. The model has an overall accuracy of 71%, providing a good prediction of massive rock where 92% of the samples are well classified. Discontinuities are worst predicted, with a ratio of well classified discontinuities, in the best case, of 14%. This result suggests that the variability of drilling parameters, as it is considered in this work, must be complemented with additional drilling data, like for instance the normalized feed pressure to detect more discontinuities. Further improvement of the recognition ability of the model, requires a better understanding of what discontinuities observed in the televiewer images have a major effect in the performance of the drilling rig.

Contents

List of Figures	3
List of Tables	6
1 Introduction	7
1.1 Thesis objective	8
2 Description of the quarry	8
2.1 Geology	10
2.2 Drilling and blasting campaigns description	11
3 Background	13
3.1 Overview of rock mass characteristics	13
3.2 Overview of measuring while drilling system (MWD) in El Aljibe	17
4 Description of the methods	21
4.1 Optical Televiewer	21
4.1.1 Borehole logging	28
4.1.2 Analysis of televiewer measurements	35
4.1.3 Characteristics of existing structures in El Aljibe quarry	40
4.1.4 Definition of a binary vector for structural characterization	48
4.2 Drilling Characteristics	50
4.2.1 MWD data processing	54
4.2.2 Discontinuity index DI	69
5 Results	71
6 Conclusion	76
7 References	78

List of Figures

1 El Aljibe quarry [7].	9
2 Location of El Aljibe quarry [8]	9

3	Temperature/pressure diagram showing the generally accepted limits of various metamorphic facies [11]	10
4	Geological map of El Aljibe [12]	11
5	Plan view showing the location of blastholes and televiewer holes.	12
6	Geometrical properties of discontinuities [14].	14
7	The dip direction and dip angel [8].	15
8	Sketch represents the types of discontinuity persistence [13].	16
9	Relation between feed force, rotation torque and penetration rate [22]	20
10	Optical Televiewer system.	22
11	The logging tool.	23
12	Optical assembly and principle of measurement [23].	24
13	Centraliser fixed on the logging probe.	24
14	Mini winch.	25
15	Mini-winch and controller [24].	26
16	Mini-winch and tripod [24].	26
17	BBox Connections with the mini winch.	27
18	Positioning of the equipment in the field [24].	28
19	Tripod with some stones to ensure stability.	29
20	Head of the televiewer with the cable connected, this connection is isolated with a tape [24] . . .	30
21	ATL Logger Suite 11.2.	31
22	Assignment of the starting depth [24].	31
23	Parameters configuration.	32
24	ATL Logger Software fully functioning [24].	33
25	Borhole image with, azimuth, gravity, magnetic field [24].	34
26	Geometric relations between the plane in the borehole (a) and the planar representation (b) [26]	35
27	Import menu.	36
28	Processing different images.	36
29	Final layout [24].	38
30	(Blast N°1, Hole N°8) Discontinuous fractures.	40
31	(Blast N°1, Hole N°2) Continuous closed fractures.	40
32	(Blast N°1, Hole N°1) Opened fractures.	41

33	(Blast N°1, Hole N°9) Voids: On the left side detected void and it is marked in grey on the right side.	41
34	(Blast N°1, Hole N°3) Filled fracture marked in purple.	42
35	(Blast N°1, Hole N°6) All area marked in Orange is considered as Weakness area.	42
36	(Blast N°1, Hole N°10) The beige line indicates the Lithology change boundary.	43
37	(Blast N°1, Hole N°1) Internal structure change.	43
38	(Blast N°1, Hole N°10) Water.	43
39	Filing material mapped [8]	44
40	Final produced image from WellCAD (Blast N°1, Hole N°8). [8]	46
41	Discontinuities by TV assessment [4]	49
42	Discontinuity from Optical televiewer assessment (Blast N°1, hole N°9).	49
43	Tamrock DX-800 top hammer rotary-percussive rig.	50
44	The in-house drill monitoring system installed in the operator-cabin(a), View of the monitoring screen(b) [28]	53
45	Flowchart showing the MWD data processing steps	55
46	Raw MWD signals (hole No. 1 in blast 1)	56
47	Density distribution of each MWD parameter for each blast. Green bars correspond to blast B1 and blue ones to blast B5.	58
48	Effect of rod addition (Blast No.1 , hole No.1) marked by a green rectangle.	60
49	MWD signals before (blue traces) and after (red traces) rod addition removal (Blast No.1 , hole No.1)	61
50	Position of the ramp-up and ending drilling modes in hole No.2 in blast B1.	63
51	Original signal (blue traces) and signal without collaring and ending effects (red traces) in hole No. 2 in blast B1.	64
52	Average signal of each MWD parameter.	66
53	Average corrected signal for RP and AP parameters.	67
54	Non normalized (blue traces) and normalized MWD signals (red traces) for the hole depth for all boreholes.	68
55	Televiewer log, and binary sequences (D_{obs} & D_{DI}) and for blasthole No. 2 in blast B1; only Fc (yellow traces), Fd (green traces), Fo (red traces) and V (grey traces) discontinuity types are considered.	74

56	(Televiewer log, and binary sequences (D_{obs} & D_{DI}) for televiewer 3 in blast B1 ; only Fc (yellow traces), Fd (green traces), Fo (red traces) and V (grey traces) discontinuity types are considered.	74
----	-------------------------------------------------------------------------------------------------------------------------------------------------------------------------------------------------------------------	----

List of Tables

1	Blasts characteristics.	11
2	Number of boreholes monitored with optical televiewer.	12
3	Description of fractures.	39
4	(Blast N°1, Hole N°3) Extracted data from WellCAD analysis.	45
5	Total N° of discontinuities and their frequencies, along with STD and mean values for each hole.	47
6	Drilling parameters under study.	51
7	General statistics about the parameters range, for raw data.	57
8	Performance of the discontinuity index formed by two parameters; a threshold percentile of 95 is obtained to build D_{DI}	72
9	Performance of the discontinuity index formed by three parameters; a threshold percentile of 95 is obtained to build D_{DI}	72
10	Recognition capacity of the DI marked in bold in (Table.8) for each discontinuity type.	75

1 Introduction

This thesis work was carried out during my stage at Escuela de Minas y Energía of Universidad Politécnica de Madrid (UPM) granted by Politecnico di Torino. The context where the study was performed correspond to El Aljibe quarry near Almonacid de Toledo (Spain), an operation based on the extraction of aggregates. The data obtained from the quarry corresponds to measurements campaigns regarding drilling, blasting and processing stages during the SLIM, "Sustainable low impact mining", project funded by the European Union, which aims to develop a cost-effective and sustainable selective low impact mining solution addressing environmental impacts, and improving flexibility, automation and safety of operations [1]. In this respect, automatization of processes in mining or civil operations provides more possibilities to the optimization, for instance, the use of cutting-edge technologies to obtain detailed rock mass characterization is important to adjust the design and improve the results from blasting and increase the overall performance of the operation, including the processing plant.

This study considers drilling data recorded by an in-house system for two blasts and direct measurements of the rock mass characteristics with an optical televiewer in 7 holes for each of these blasts. The optical televiewer provides a detailed rock mass characterization that allows a better understanding of the variations and changes of MWD system parameters. In this work, borehole images of different boreholes were interpreted and processed through WellCad software to identify and mark the fractures and discontinuities after that a binary vector was built. Drilling data of different operational parameters were filtered in several steps through MATLAB 2021. Variability of these data are considered to calculate a Discontinuity index [2]; [3]; [4] that has been calibrated with the binary vector obtained from borehole inspection with Optical televiewer data. To achieve this objective, different scripts have been written in [5].

1.1 Thesis objective

The goal of this study is to develop a model to recognize discontinuities from drilling data based on the classical discontinuity index [2];[3]. For this, the position and characteristics of discontinuities observed from televiewer logs are used to define the parameters included in the index and their weight to assess the prediction ability of the model. To generate a virtual core representing the structural condition of the rock a binary sequence, where ones describe discontinuities and zeros massive rock, is built from the discontinuity index and compared with the sequence obtained from the televiewer inspection (presence/absence). A proper rock mass characterization is an important requirement to have an effective control of the production cycle [6]. It is essential for efficient blasting and fragmentation, detecting discontinuities to adapt the explosive charging, for instance, areas of heavily fractured rock could be charged with explosives with less energy while for areas with massive rock higher energy explosives is required. Additionally, in the case of blastholes with big cavities that will cause loss of explosives, charging with bulk explosives could be avoided and another alternative, such as liners, is used.

2 Description of the quarry

El Aljibe quarry is an open pit for extraction of aggregates. The aggregates are mylonite which is a metamorphic rock. Benito Arnó e Hijos S.A.U. owns the exploitation, that has been functioning for over 12 years. The exploited material is ideal to produce rail ballast (32-56 mm) and pellets for highway asphalt agglomerates due to its wear resistance and fragmentation characteristics (6-12 mm). Figure 1 shows an overview of the quarry. El Aljibe quarry is located close to Almonacid de Toledo (Castilla-La Mancha, Spain), a small town 100 km far away from Madrid (see Figure 2).



Figure 1: El Aljibe quarry [7].



Figure 2: Location of El Aljibe quarry [8]

2.1 Geology

The rocks mined in El Aljibe quarry are part of a metamorphic belt that is 1-1.5 km long and 400 meters high . This belt reacts to a ductile shear zone formed during the Hercinian Orogeny's final tectonic event [9]. The mylonite and cataclasite series were formed as a result of this geological structure (see Figure 3). Ultramylonite , orthomylonite, ultracataclasite, and protomylonite are the principal lithologies found at the mine site . Orthomylonite, a magnetic protholyte mylonite, is the most common rock type in the El Aljibe quarry. Tectonic forces shaped it, and it has a density of 2.71 t/m³ and is extremely hard with a Uniaxial Compressive strength and tensile strength of 171.27 MPa and 18.21 MPa, respectively [10]. Figure 4 shows the location of the quarry in the geological map.

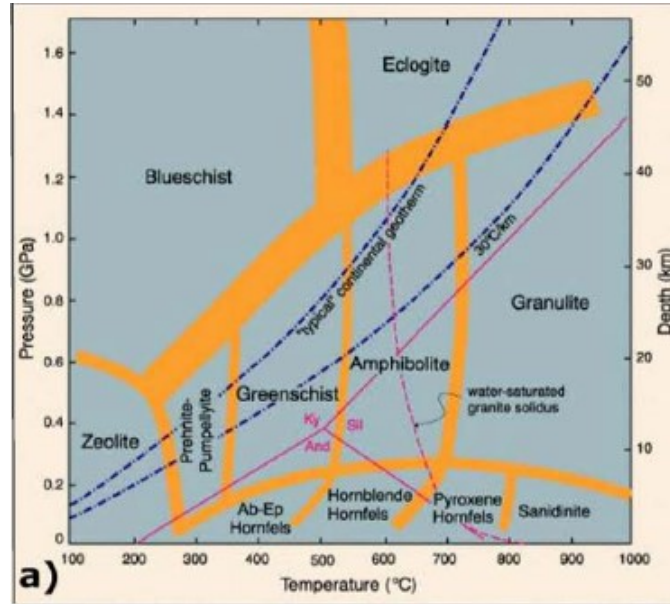


Figure 3: Temperature/pressure diagram showing the generally accepted limits of various metamorphic facies [11]

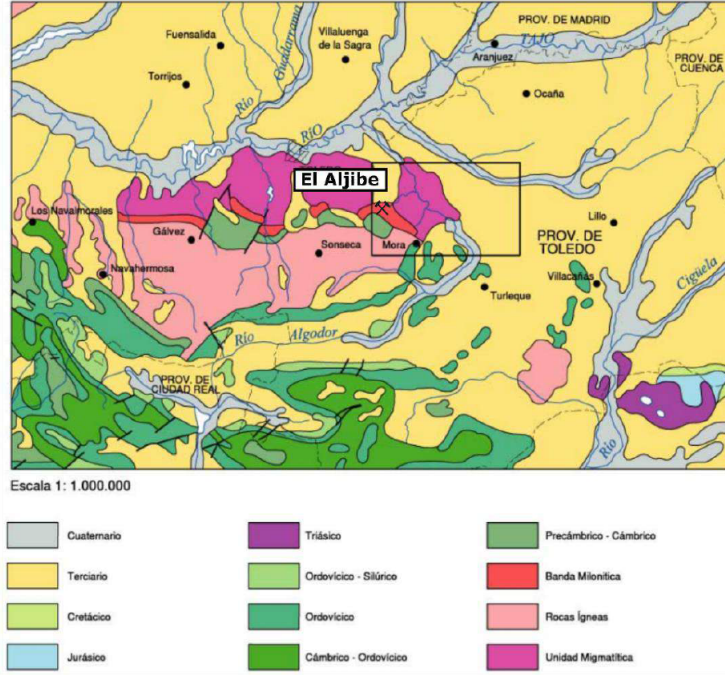


Figure 4: Geological map of El Aljibe [12]

2.2 Drilling and blasting campaigns description

Two drilling and blasts campaigns, named B1 and B5 executed in 2018 were considered in this study. The blasts were made up of one row of seven blastholes. A Tamrock DX-800 equipped with an in-house Measuring-while Drilling (MWD) system was used. The holes had a diameter of 89 mm and an inclination about 16° . Table 1 summarizes the main characteristics of the blasts. The explosive was a double salt emulsion that was bottom initiated with 4 ms electronic detonators.

Table 1: Blasts characteristics.

Blast id.	B1	B2
Burden (m)	2.4	2.9
Spacing (m)	3.2	3.2
Bench height (m)	11.5	11.9
Total powder factor (kg/m3)	0.93	0.81

In these two blasts, additional holes called televiewer holes were drilled closed to the blastholes to analyze rock damage. The configuration of blasts B1 and B5 is shown in Figure 5. Blue and red are points used to indicate blastholes and televiewer holes, respectively. The optical televiewer was not used to measure the blastholes shown in green. Table 2 summarizes the number of boreholes monitored with the optical televiewer.

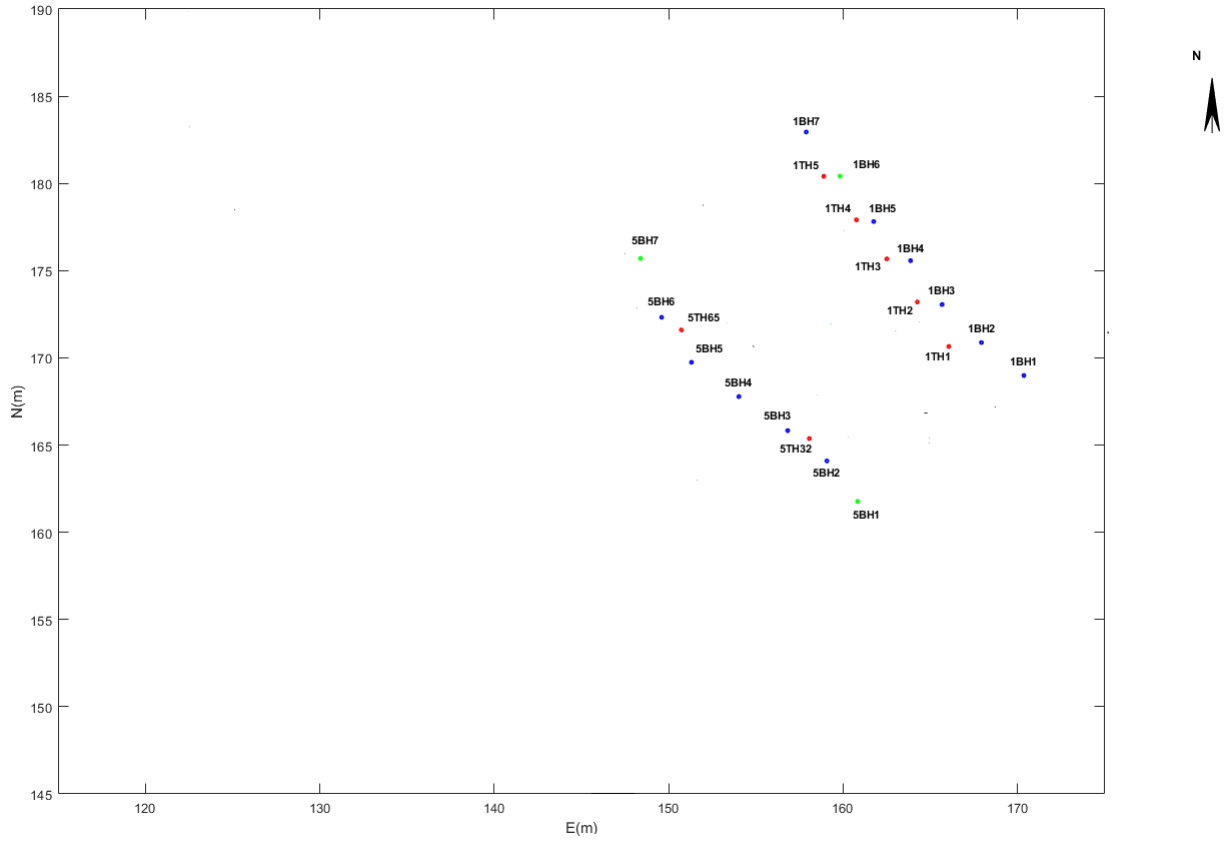


Figure 5: Plan view showing the location of blastholes and televiewer holes.

Table 2: Number of boreholes monitored with optical televiewer.

Blast N°	No. Blastholes	No. Televiewer holes
B1	6	5
B5	4	2

3 Background

This section reviews the basic characteristics of discontinuities and their effect on the rock mass characteristics. Also is describes the state of the art of the MWD technology and the effects of the rock conditions on the response of the drill.

3.1 Overview of rock mass characteristics

Because the rock masses that make up the earth's surface are crossed by bedding planes, primary foliation, planes of schistosity, fractures or joints, these discontinuities impact the mechanical behaviour of the rock mass, and thus this causes a response of the drill rig when it reaches a discontinuity. Natural forces applied to a rock mass over time can have a variety of impacts, such as deformation and distortion, or fractures if the strength of the rock materials is exceeded. In all circumstances, a number of chemical and physical elements influence the deformation's outcome [13]:

- The speed with which the deformation occurs
- The degree of confining pressures
- Temperature
- The existence of pore fluids and their pressure
- The strain forces severity
- The pace of application of the deforming forces

Discontinuities can be classified into two groups: relevant discontinuities (scale of centimetres), which can create an effective variation in rock mass behaviour, and integral discontinuities, which do not. Foliation in gneisses induced by mineral segregation into different bands, or changes in grain size and mineral content observed in sedimentary rocks, could cause an integral discontinuity [13]. Weathering or changes in stress conditions can cause this type of discontinuity to become mechanically relevant: for example, in some metamorphic rocks, weathering of

their internally aligned mineral grains can cause noticeable mechanical discontinuities. Weathering can be exacerbated by other variables, such as stress release, resulting in displacement and distortion. Other causes, such as cementation or mineralization, can, on the other hand, cause a conspicuous discontinuity to transform into an integral discontinuity.

A critical factor to consider in blasting is identifying and analyzing discontinuities features. According to Torres [14], the five most important geometrical properties of discontinuities for engineers are, spacing, aperture (gap) , orientation, persistence, and roughness these are shown in Figure 6 . Among them spacing and orientation with respect to the highwall face are the parameters usually considered in fragmentation prediction models [15] and [16]; [17]. Their main characteristics are defined next:

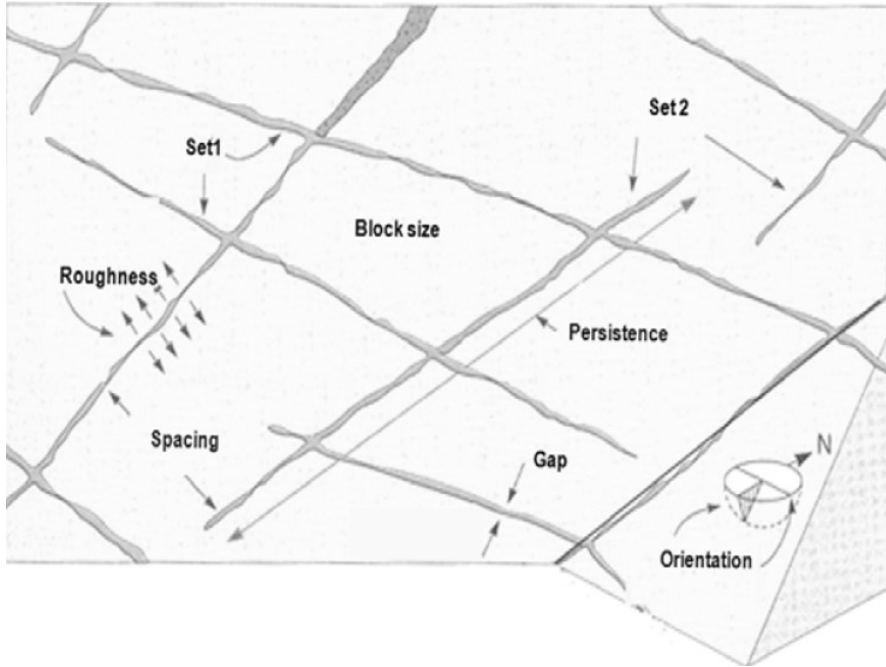


Figure 6: Geometrical properties of discontinuities [14].

◆ **Spacing:** The distance between discontinuities or spacing provides a trend in the mechanical behaviour of the rock mass and defines the maximum block. Set spacing, total spacing, and standard set spacing are three ways to measure spacing [13]. Set spacing refers to the distance between joints in the same family or set. Total spacing is the distance calculated along

a scanline between two contiguous discontinuities while for standard set spacing, the scanline must be perpendicular to the set's average orientation.

◆ **Aperture:** The distance between discontinuity's faces determines its opening. Because of the presence of filling material, water, or air, the aperture has a significant impact on the joint's shear resistance. Displacement along the discontinuity can result in significant opening.

◆ **Orientation:** It is made up of two components, the dip direction which is the line perpendicular to the plane's horizontal intersection and represents the azimuth value, it is measured clockwise from the actual north direction and ranges between 0° to 360° (see Figure 7), and the plane's maximum declination with respect to the horizontal, measured in degrees between 0° (horizontal planes) and 90° (vertical planes), is referred to as the dip angle and it is the second component and measured [13]. When two components are measured the plane orientation can be defined for example ($200^\circ/00^\circ$).

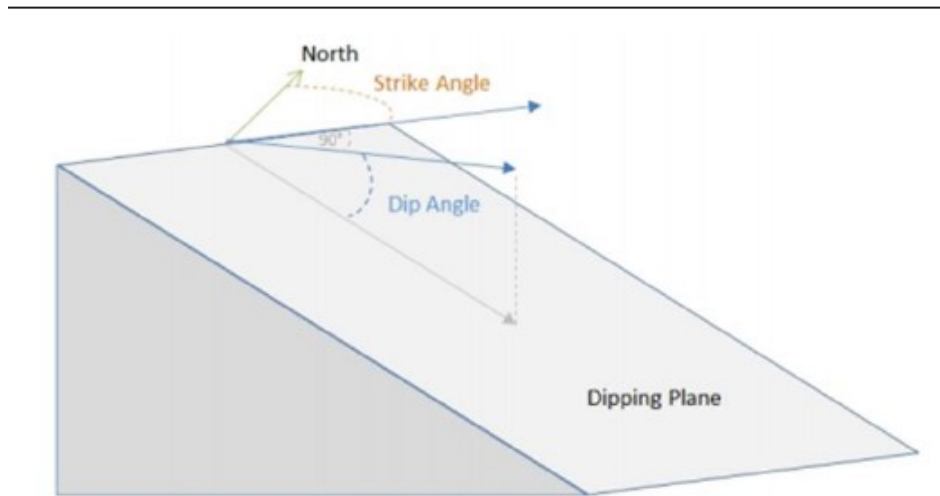


Figure 7: The dip direction and dip angel [8].

♦ **Persistence:** Represents the extension and continuation of a discontinuity in every direction. Persistence is defined according to where a discontinuity ends [13], as the following (see Figure 8) for a graphical definition as well:

- Non persistence discontinuity, at the which the plane of discontinuity ends within the intact rock.
- Persistence discontinuity, the planes are extending in every direction of the same face of the rock.
- Abutting discontinuity, it is when a discontinuity ends at another discontinuity.

The persistence of a discontinuity has an enormous effect on the mechanical behaviour of a rock, for instance non persistence discontinuity can obstruct or disallow the movement of a certain blocks, until the discontinuity extends and reaches another blocks.

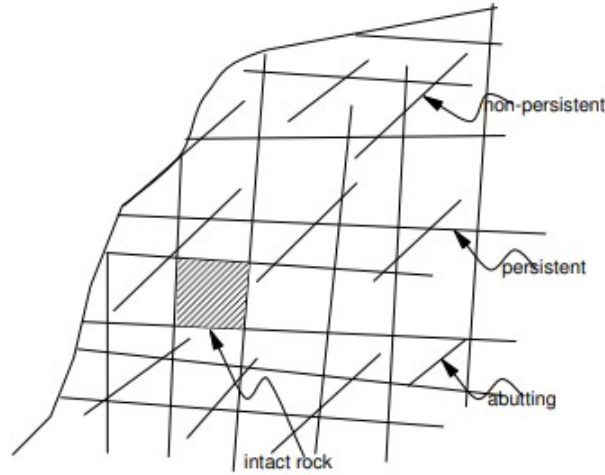


Figure 8: Sketch represents the types of discontinuity persistence [13].

♦ **Roughness:** could be considered as a measure of shear strength along discontinuities and it is the surface irregularities on the plane of a discontinuity, therefore the term roughness requires two observations scales [13]: millimetric and metric scales and because testing on-site is impracticable due to the large diameters of the surfaces, the shear strength must be computed using roughness. Minor scale asperities rule small displacements, while large scale asperities govern big displacements .

3.2 Overview of measuring while drilling system (MWD) in El Aljibe

Drilling monitoring systems collect digital signals from multiple factors involved in the drilling process using sensors positioned along the various operational mechanisms of the drilling machine, such as the boom and drill rod to capture digital signals from a variety of parameters involved in the drilling process. The (MWD) technique is a drill monitoring system that logs drilling data at predetermined length intervals, providing information on the drilling's operating characteristics [18]. This technology provides real-time measurements of operational parameters from drilling rigs, which can be thought of as the response of the rock mass during this operation. The fact that the technology delivers data with high resolution and low production disturbance made it a useful supplement for the characterization of rock masses [6].

The performance of the rig is monitored in real-time by sensors installed at different locations of the rig. Those sensors are associated with the rotational, flushing, and percussive operations controlled by the drill rig [6]. The drilling management is performed by a control system that modify the drilling pressures values to fully optimize the operation and minimize bit wear or eliminate any damage that can happen to the drill rig [18].

For rotary-percussive drilling, the parameters of MWD can be categorized as dependent or independent with respect to the effect of geological characteristics in the of rock mass in the drilling bit, hence due to the adjustment of the system, these parameters are grouped as independent parameters, that corresponds to the ones can be controlled directly by the operates and includes:

♦ **Feed pressure (FP):** It is the pressure of the fluid driving the machine that keeps the bit in

contact with the rock while the system percussion and rotation. In other words, it is a measure of the normalized thrust with the diameter of the drill in (bar).

- ◆ Rotation speed (RS): it is considered as the number of turns of the bit per minute.
- ◆ Percussive pressure (PP): or head pressure (bar). It is the real pressure exerted by the drill in its most advanced part and measured with head sensors.
- ◆ Damp pressure (DP): represents the measured pressure at the end of the bit stroke to prevent unwanted vibration or drill string movement in (bar).

Then, the dependent parameters, corresponds to those could be dependent on the previous parameters and on the rock characteristics:

- ◆ Penetration rate (PR): penetration rate (dm/min). Relationship between the depth and the time interval immediately after the last datum. According to studies, it is influenced by the geomechanical response of the rock [18] and by the independent parameters FP, PP and RS.
- ◆ Rotation pressure (RP): Torque applied by the rotation motor. It is usually given in bar and is understood as the resistance exerted by the rock to the rotation of the machine. According to studies, it is influenced by the type of rock, the design of the bit, and the independent parameters FP and RS [19]. It can increase with depth due to friction on the drill rod and hole wall.
- ◆ Air pressure (AP): It relates to the amount of water (or sweep fluid) that enters the hole, with which the drill cuttings are expelled to the surface. Variations in this parameter facilitate the prediction of fractures and holes.

The following are some of the most important relations discovered in previous research:

- The feed pressure (FP) considered as an independent parameter maintains the contact between the bit and the bottom of the hole to ensure an optimum penetration rate (PR). Figure 9 shows that the penetration rate increases with the increment of feed pressure until a maximum point . From this point, any further increment in the feed pressure will influence the penetration rate and causes a drop in (PR) [18]. On the contrary, unexpected decrease in the feed pressure makes the penetration rate to increase significantly as a result of the advance of the bit without energy being transferred to the rock, such a situation

happens while drilling through a cavity or big discontinuity.

- The use of excessive feed pressure in weak rock (highly jointed) obstructs the functioning of the rod, preventing the bit to cut the rock efficiently due to the cuttings that cannot be removed by the flushing fluid. As a result a decrease in the penetration rate takes place [20]. [21], defining the optimum feed pressure as the value that provides penetration rates near to the maximum, ensuring that the bit is always in contact with the bottom of the hole and no excessive pressure is being performed.
- The rotation pressure is important for drilling as it is associated with how much is the has resistance to wear and the friction with the rod and hole walls [20]. The values of rotation pressure at high penetration rates tends to drop [20]. In this regard, low penetration rates are usually associated with rock that has high resistance (hard rock), that causes an increase in the rotation speed. On the contrary, very weak rock with less resistance increases the penetration rate and consequently the rotation speed decreases. Additionally, the two parameters PR and RP are identified as parameters that respond to considerable to changes in the rock mass caused for instance by the existence of discontinuities.

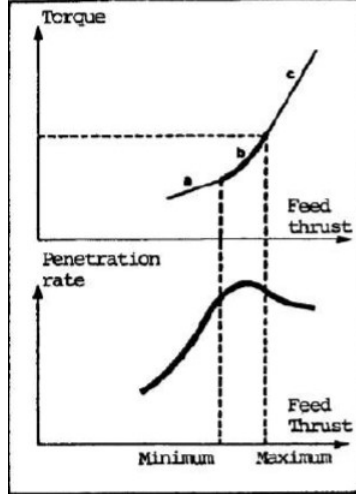


Figure 9: Relation between feed force, rotation torque and penetration rate [22]

Despite, both independent and dependent drilling parameters react to rock features or changes in rock strength, the dependent drill parameters have been widely employed to make correlation with rock properties. The relation between measuring while drilling parameters and rock mass characteristics is not fully known or understood, and there is no uniform model or formula based on MWD that can be used at any location.

4 Description of the methods

Two different technologies for assess rock mass condition are considered for this study, MWD system and optical televiewer. The optical televiewer is for rock mass characterization providing accurate information on the position of discontinuities and of their orientation and aperture. It causes, however, a disruption in production as the setting up of this equipment in the field takes about 30 to 45 minutes, considering the logging of about 12 m depth per hole. On the other hand, MWD system provides online measurements of the rig performance while drilling. This data, however, do not provide any direct information of the rock mass characteristics if is not correlated with direct measurements of the rock mass, such as those obtained by the optical televiewer, to define an index by a combination of operational parameters that predict some rock condition or property of interest.

4.1 Optical Televiewer

The logging tool, the data collection system, the mini-winch with 200 m of 1/8" wireline, and a computer with the software ATL Logger Suite 11.2 make up the major components of Advance Logic Technology's optical televiewer (see Figure 10). The optical borehole televiewer probe provides 360° oriented colour image of the hole wall. The logged images are processed and analysed with the software WellCAD (Advanced Logic Technology).



Figure 10: Optical Televiewer system.

The main characteristics of the system components are described next:

◆ **The logging tool:**

The logging tool with a length of 1.47 m, weight of 5.3 kg and a diameter of 40 mm, has a bottom-mounted imaging system, a centre section with hole surveying sensors to measure the azimuth and the dip of the hole, a top-mounted wireline connector, and two centralisers (see Figure 11) suitable for 89 mm boreholes [23].



Figure 11: The logging tool.

This tool includes a CMOS (complementary metal-oxide-semiconductor) digital image sensor with 1.2 Mpx and fisheye matching optics (see Figure 12) . Ten LEDs serve as the light source. The displayed log image is created by extracting a single annulus from the active pixel array. Azimuthal resolutions of 120, 180, 60, 600, 900, and 1800 pixels per revolution are available. Vertical resolution is a function of depth encoder vertical resolution and is essentially the vertical size of a pixel. The azimuthal resolution was set to 900 px and the vertical resolution to 1 mm. The whole surveying system is composed by three axis magnetometers and accelerometers, with an accuracy of $\pm 1.2^\circ$ in azimuth and ± 0.5 .

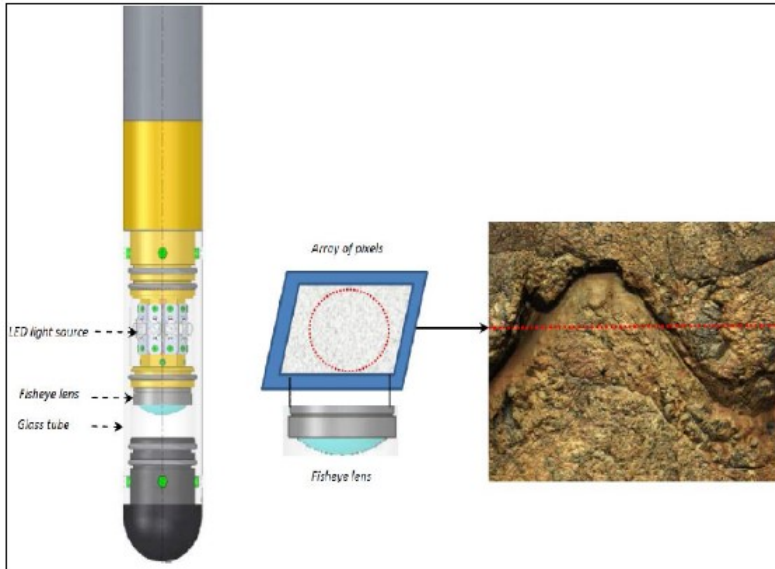


Figure 12: Optical assembly and principle of measurement [23].

The centralisers that ensure that the system is properly centered in the borehole, are made up of four nonmagnetic blades that are arranged in two rings one is stable, while the other moves along the tool to respond to abnormalities in the borehole walls (see Figure 13).



Figure 13: Centraliser fixed on the logging probe.

♦ **The mini winch :**

The mini winch has a cable that is made up from steel and connected to the logging tool. It allows moving the logging tool along the borehole at a steady speed, powers the probe and allows data exchange. The miniwinch has a weight of 38 kg and a size of $66 \times 46 \times 46$ cm (see Figure 14). It has a precise measurement wheel and a rotary encoder that can track the depth of the logging tool. This instrument can control rising and descending velocities, and the system includes a clutch that breaks the probe, allowing it to remain still at a constant depth (see Figure 15).



Figure 14: Mini winch.

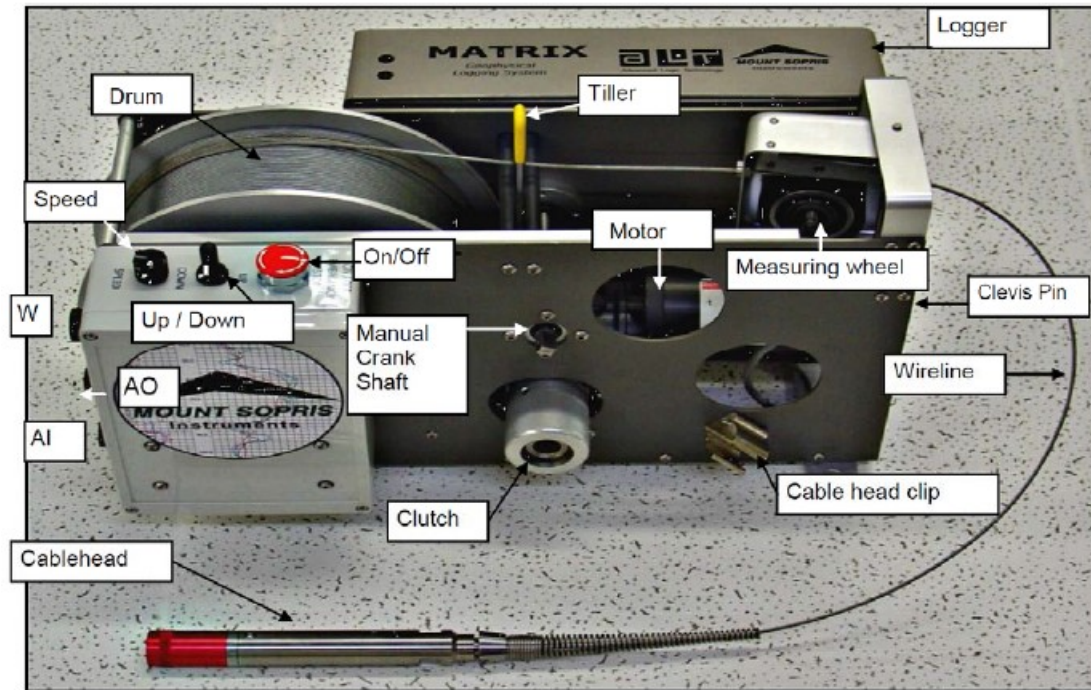


Figure 15: Mini-winch and controller [24].

To allow the logging tool to be in a good position in the borehole while connected to the mini winch and to guide it along the borehole a Tripod is used, the tripod as well reduces the stress on the wire-line (see Figure 16) .



Figure 16: Mini-winch and tripod [24].

◆ **Data acquisition system :**

The miniwinch is attached to an acquisition system that serves as a link between the logging tool and the computer, using the ATL Logger Suite software (see Figure 17).



Figure 17: BBox Connections with the mini winch.

◆ **Computer:**

A computer with the software ATL Logger Suite software controls the tool stores and displays the images of the borehole wall.

4.1.1 Borehole logging

Normally it takes at least half an hour to put together the essential equipment to conduct field research. The tool has two functioning modes, in ascending logging the resolution and speed is 900 pixel per revolution and 1.0 m/min, while for descending mode is 300 pixels per revolution is and 2.4 m/min, respectively. Sometimes boreholes diverge from intended trajectories, this causes the televiewer to come to a standstill position in the borehole, preventing continued surveying. In this scenario, the winch must be used to draw it up and down [24].

The following steps describe the process in the field:

- Place the equipment (i.e. miniwinch, data acquisition system and generator) in the centre of the boreholes that will be examined. This is critical to avoid undue strain on the wire-line. Place some stones in front of the winch to halt it, and prevent that it can moved if the logging tool is stacked in the hole (see Figure 18) .



Figure 18: Positioning of the equipment in the field [24].

- Connect the computer and the winch to the data collecting system; each cable should be connected to a single entry to prevent data from being mixed up.
- Fix the tripod and put it behind the hole to be measured and secure it. The tripod should be stable and no movement is allowed (see Figure 19), the same applies to the mini winch to avoid stress in the wire-line.



Figure 19: Tripod with some stones to ensure stability.

- Set up the logging tool starting with fixing the centralisers to the desired hole diameter. Connect the logging tool to the wireline and use a tape to safeguard the connection (see Figure 20).



Figure 20: Head of the televisioner with the cable connected, this connection is isolated with a tape [24]

- Turn the electricity generator on. The data collection unit should then be started.
- Put the logging tool inside the borehole,. This operation requires two people to avoid the logging tool's camera colliding with the borehole walls.
- Connect the program ATL Logger Suite 11.2 in the computer (see Figure 21) to control the logging tool.

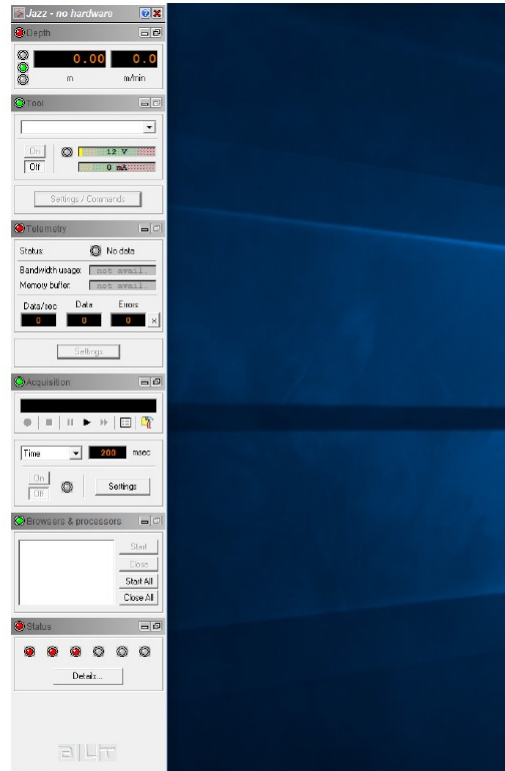


Figure 21: ATL Logger Suite 11.2.

- Using the winch control system, to place the top part of the logging tool defined by the isolating tape at the height of the borehole collar. On the software a window showing depth will appear and the depth shown should be around 1.5m, which is the length of the probe (see Figure 22).

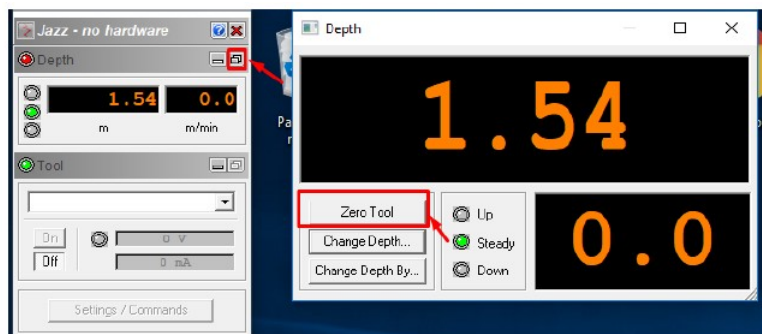


Figure 22: Assignment of the starting depth [24].

- After defining the borehole diameter, resolution, azimuth, depth and light intensity (see Figure 23) scanning down the hole will start. At around depth of 0.5m from the bottom of the hole, the logging tool should be stopped to protect the glass at the end of the logging tool from colliding.

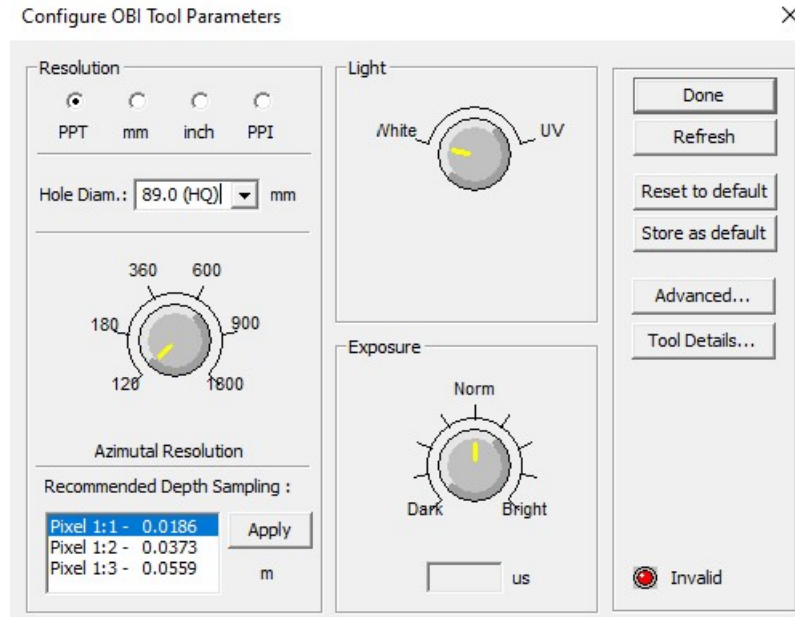


Figure 23: Parameters configuration.

- Prepare the ATL logger software to begin recording. For this, save the file with the following information: "date, borehole number, starting depth off recording, direction, pixel resolution, and field of view.
- The speed of the winch should be fixed to ensure that the buffer is below a certain percentage (90%) that allows a proper data exchange between the logging tool and the computer. This usually occurs for a velocity of 1 m/min according to the desired resolution.
- Fix the acquiring resolution to 900 pixels per turn and the brightness to match the image from the descending surveying.
- Click record and start recording while the tool is ascending through the borehole.

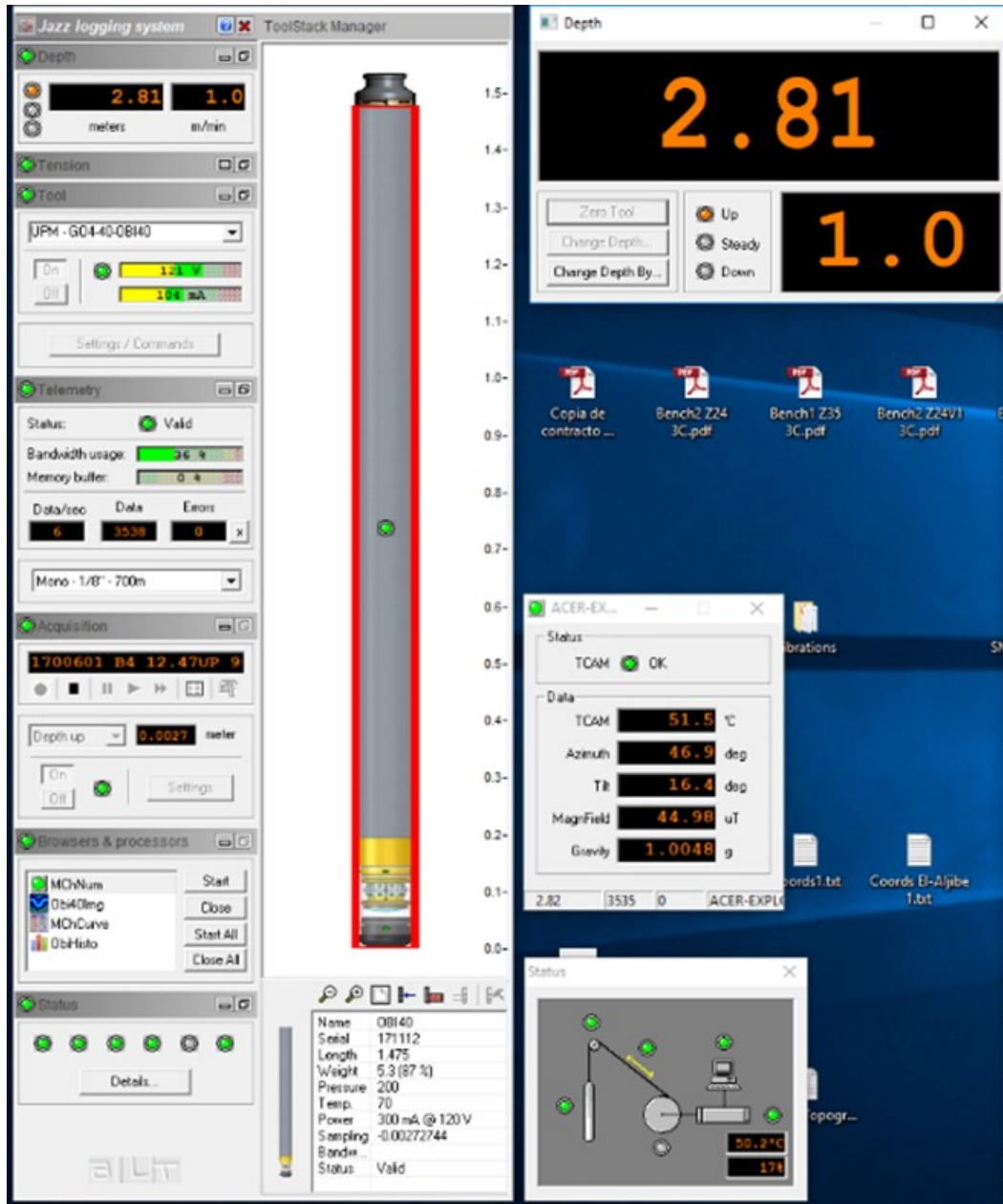


Figure 24: ATL Logger Software fully functioning [24].

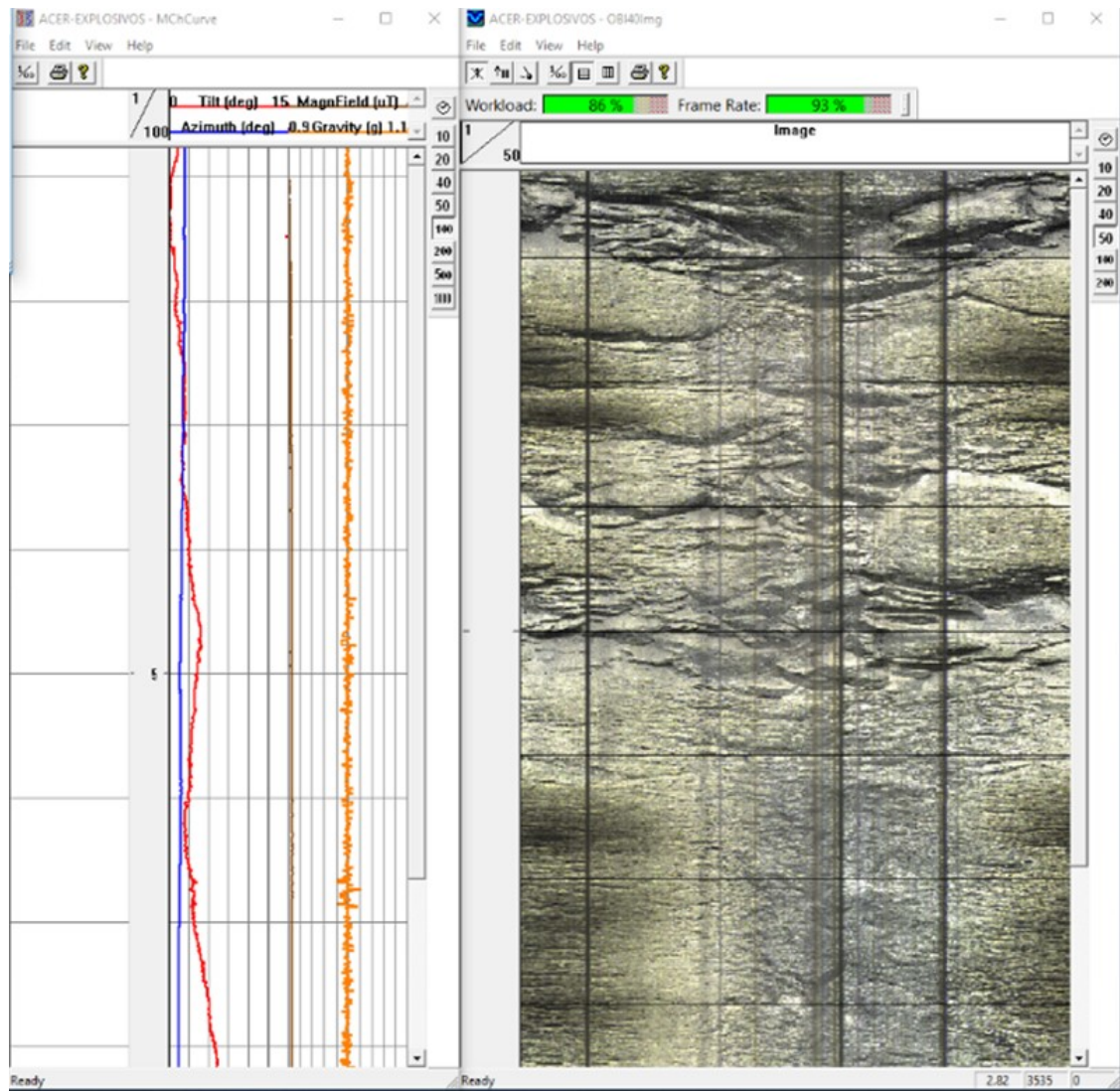


Figure 25: Borehole image with, azimuth, gravity, magnetic field [24].

- Stop recording when the top part of the probe reaches the collar of the borehole.
- Turn off the logging tool and carry out the same steps for a second borehole.

4.1.2 Analysis of televiewer measurements

All examined boreholes receive a log file with the extension `tfd` from the ATL Logger Suite 11.2 software that can be opened and processed through WellCAD software. The software shows the `tfd` file as a cylinder and display the borehole wall in a plane. When projected, the elliptical discontinuity traces formed by planes intersecting a cylinder are described by a sinusoidal wave. From the amplitude and the coordinates of three non-collinear points of the trace, WellCAD calculates the dip α and the dip direction β (see Figure 26), [25] for more details on the formula used.

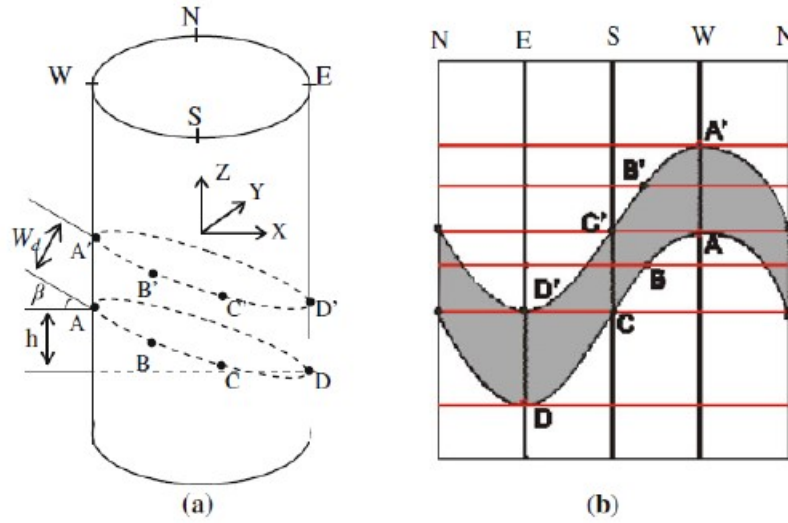


Figure 26: Geometric relations between the plane in the borehole (a) and the planar representation (b) [26]

The following steps describe the use of the WellCAD software:

- ◆ Select the relevant log files for the borehole of interest from the file menu, import a single File (see Figure 27).

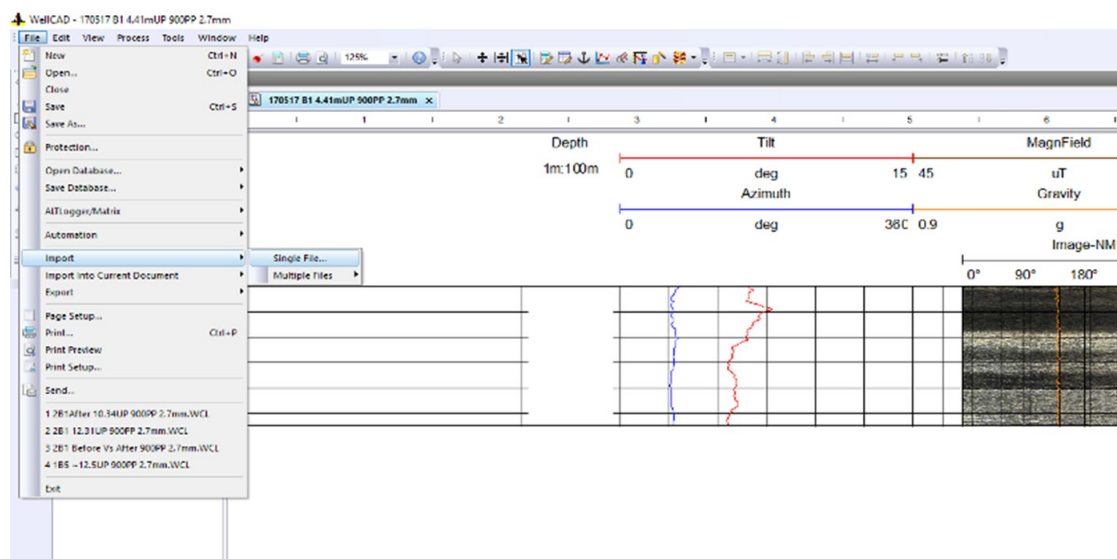


Figure 27: Import menu.

◆ It is possible to import a new log into the same file, this is particularly beneficial when borehole logging has been suspended, as it enables the integration of several files from a borehole log into a single model (see Figure 28).

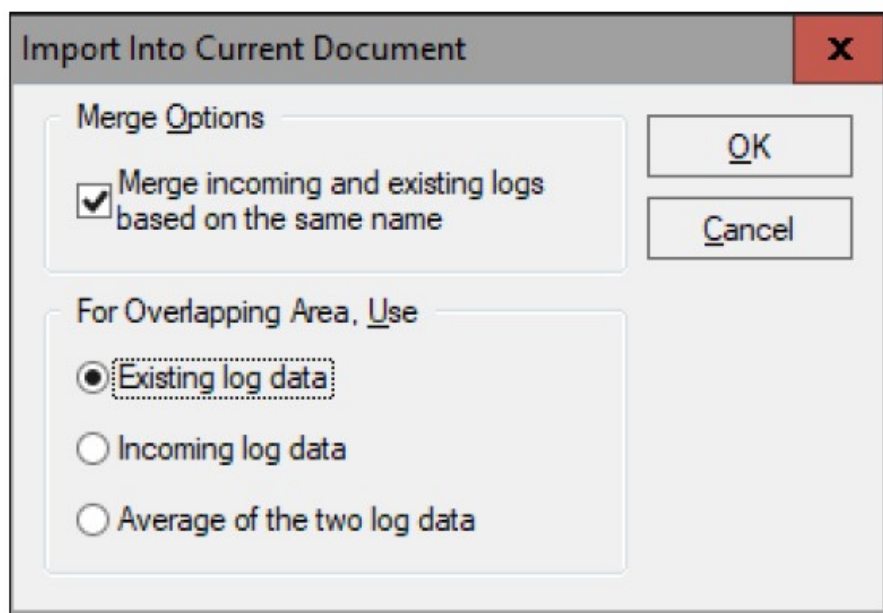


Figure 28: Processing different images.

◆ At each depth, the tilt, azimuth, magnetic field, gravity, and picture are displayed after the file is opened (see Figure 29).

◆ Once the image is displayed and everything is set, the first step is to enhance and formulate the presentation of data and to do this, we follow these steps:

1. Change the units to mm by double click on the ruler.
2. Defining the scale by clicking on the depth header, the scale is usually (1m:10m or 1m:20m), to clearly visualize the discontinuities.
3. Click on the tilt header while pressing the control key (Ctrl) and choose azimuth, magnetic field and gravity and then press on the align left and right button consequently the logs will be stacked.
4. After clicking on the depth header and while pressing the control key (Ctrl) click on azimuth, tilt, magnetic field, and gravity after that on the document layout (on the top part of the screen) press insert after, to put the logs immediately after depth.
5. On the tilt header while pressing the (Ctrl) button select Image-NM and on the document layout press insert after, to position the chosen logs after depth.
6. To remove the depth grids, we go to the setting in Image-NM, this will make the process of marking the fractures easy.

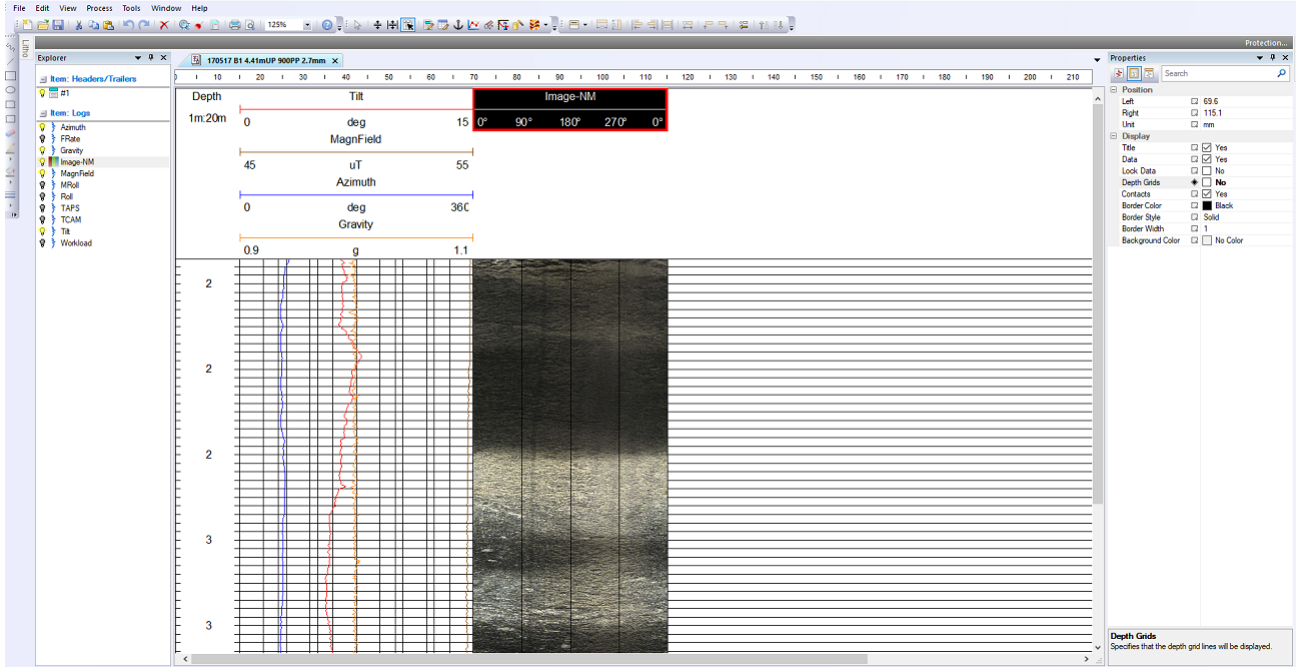


Figure 29: Final layout [24].

◆ A copy of the Image-NM should be created, after that click on the desired image header to start removing the noise and image filtering through these steps:

1. Process menu ➤ Image Module menu ➤ RGB Module menu ➤ interpolate bad traces, to remove bad traces.
2. Process menu ➤ Image Module menu ➤ RGB Module menu ➤ Adjust Brightness and contrast, press on auto in the histogram to improve the image.

◆ Once everything is set the next step is to mark discontinuities. This step starts creating a new structure log with a new name that will be placed under the image. Then click on the setting menu to update the structure style in the new structure log to projections. The borehole log already contains a description of the fractures and structures to be marked. Once a structure is found while scrolling through the image is fitted with sinusoidal trace according to their code and colour described in Table 3.

The first four discontinuity types with the codes (Fd, Fc, Fo and V) shown in Table 3 are considered for this study as they likely involve large fluctuations in the response of the drill

rig [20] playing then a major role in blasting.

Table 3: Description of fractures.

Criteria	Name	Code	Colour
Discontinuous fractures or fractures that are difficult to recognize at first look	Discontinuous fracture	Fd	Green dashed
The continuous fracture is immediately identifiable.	Continuous closed fracture	Fc	Yellow
A continuous crack with a discernible opening	Opened fracture	Fo	Red
A Caves or natural cavities with loosing material	Void	V	Grey
Fracture filled with sediments	Filled fracture	Ff	Purple
Low resistance area due to rock structure(e.g Foliation)	Weakness area	W	Orange
Lithology change	Lithology	L	Beige
Internal structure change (e.g stratification, viens)	Structure	S	Pink
Water presence	Water	Wt	Blue
Area with non-compacted material	Fill	Fill	Dark grey

4.1.3 Characteristics of existing structures in El Aljibe quarry

The fractures were categorized based on their continuity and opening. This section will describe these fractures

◆ Discontinuous fractures:

Partially fractured structures occur when the sinusoidal trace is visible in 50 to 75% of the lateral surface of the borehole wall (see Figure 30).

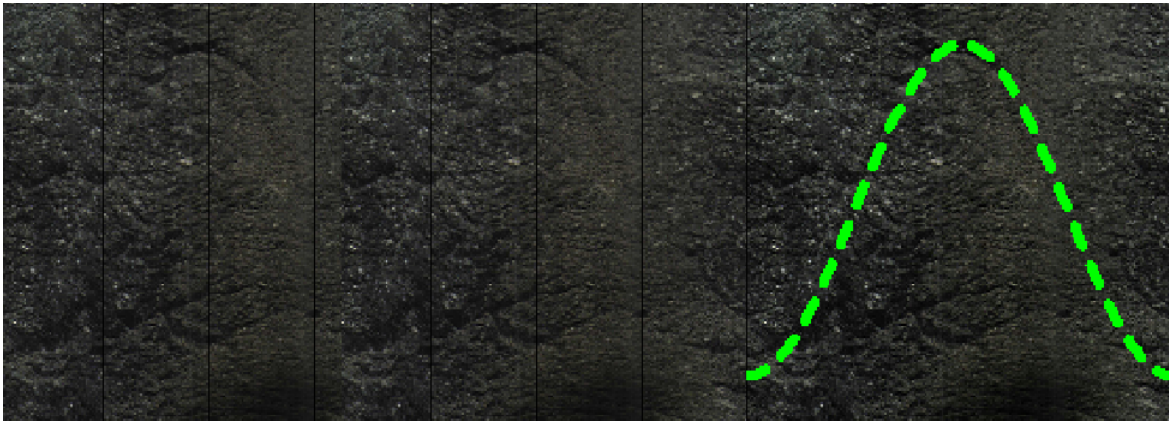


Figure 30: (Blast N°1, Hole N°8) Discontinuous fractures.

◆ Continuous closed fractures:

The trace of continuous closed fractures is distinct and visible in 100% of the lateral surface of the borehole wall (see Figure 31).



Figure 31: (Blast N°1, Hole N°2) Continuous closed fractures.

◆ Opened fractures:

An example is shown in Figure 32.

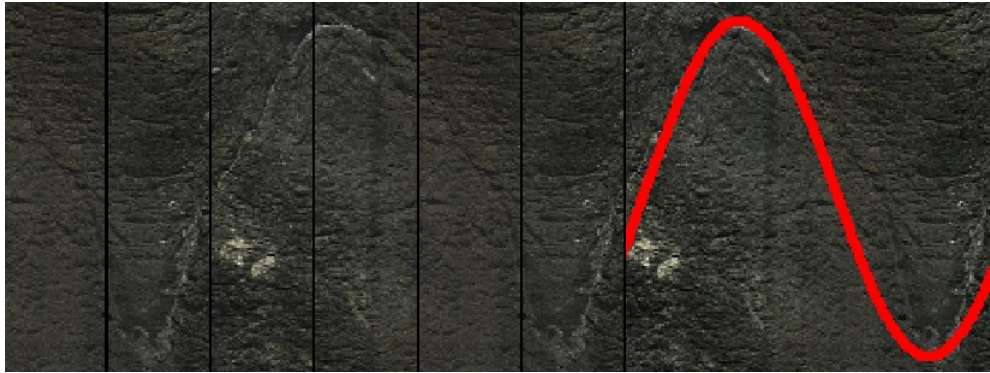


Figure 32: (Blast N°1, Hole N°1) Opened fractures.

◆ Voids:

Rock detachment cause voids specially during the drilling process (See Figure 33).

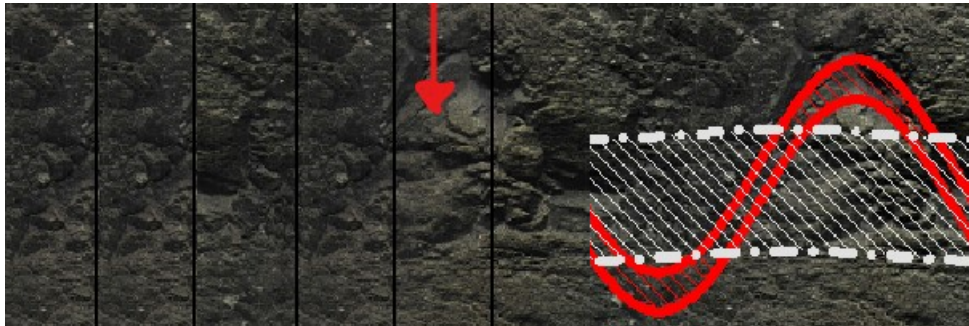


Figure 33: (Blast N°1, Hole N°9) Voids: On the left side detected void and it is marked in grey on the right side.

◆ Filled fractures:

These fractures open and characterized by a filling material that could be of non-consolidated material (see Figure 34).

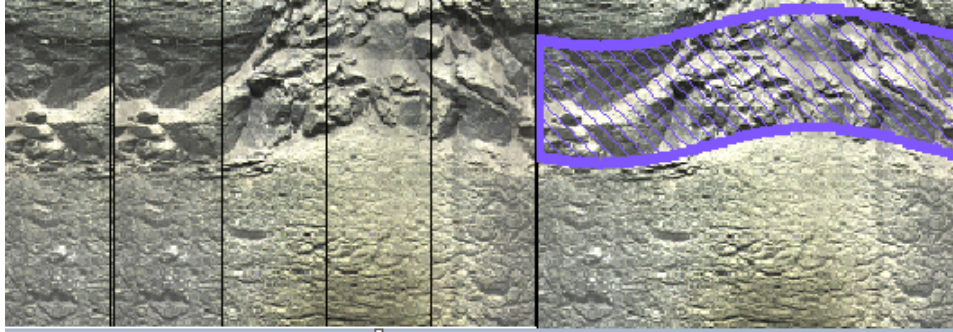


Figure 34: (Blast N°1, Hole N°3) Filled fracture marked in purple.

◆ Weakness area:

Those are areas where the rock is weak and has the lowest resistance (see Figure 35).

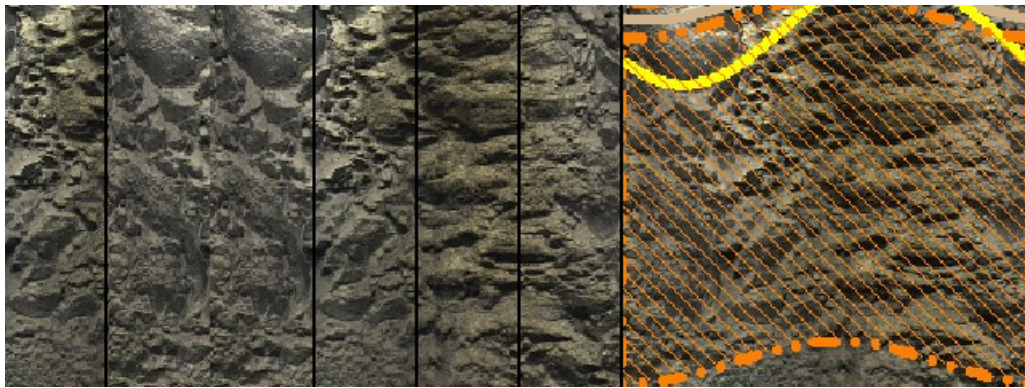


Figure 35: (Blast N°1, Hole N°6) All area marked in Orange is considered as Weakness area.

◆ Lithology change:

Variations in rock color and internal structure can be noticed. Thus we can classify the zone as change in lithology (see Figure 36) .

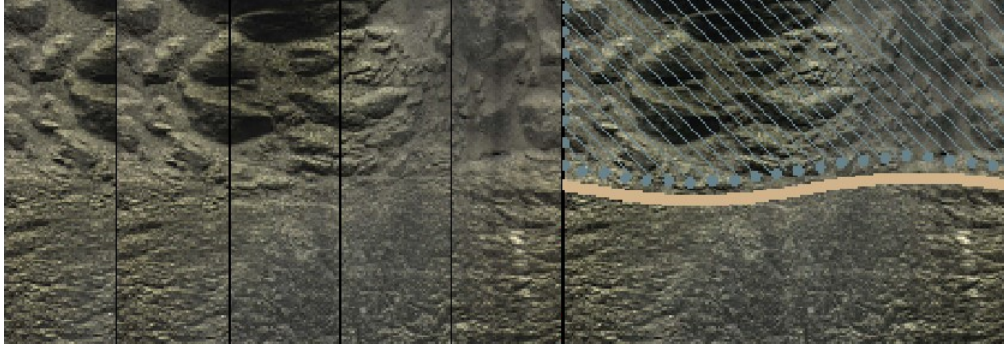


Figure 36: (Blast N°1, Hole N°10) The beige line indicates the Lithology change boundary.

◆ Internal structure change:

Figure 37 shows an example of flotation, veins, and bedding planes.

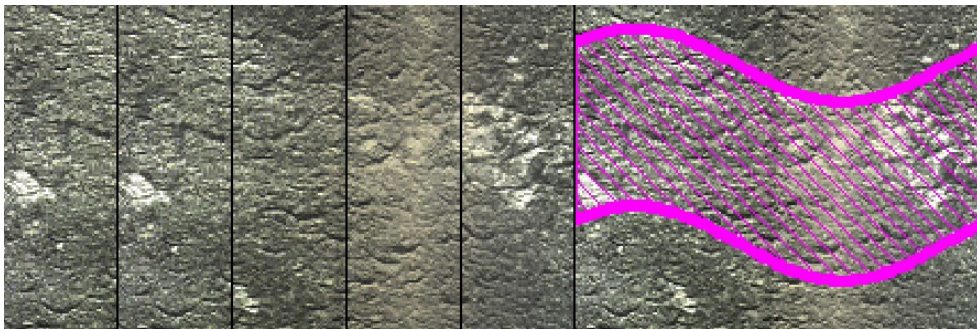


Figure 37: (Blast N°1, Hole N°1) Internal structure change.

◆ Water:

The presence of water is mapped and recognized, this is shown in Figure 38

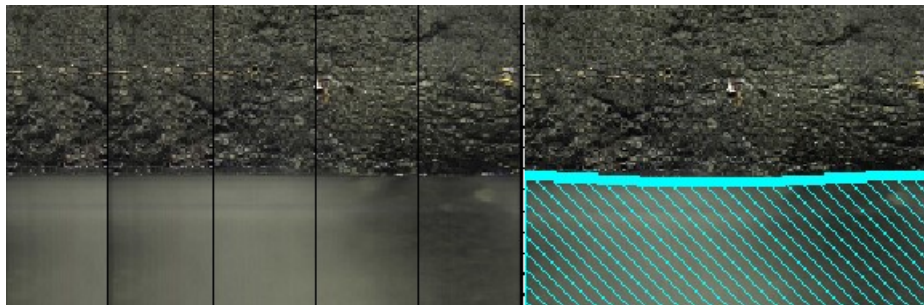


Figure 38: (Blast N°1, Hole N°10) Water.

◆ Fill:

The covering cloth on the bench's top is an example of this feature (soil or filling material), but usually it is hard to be detected because of their very small thickness in comparison with the length of the logging tool (see Figure 39) .

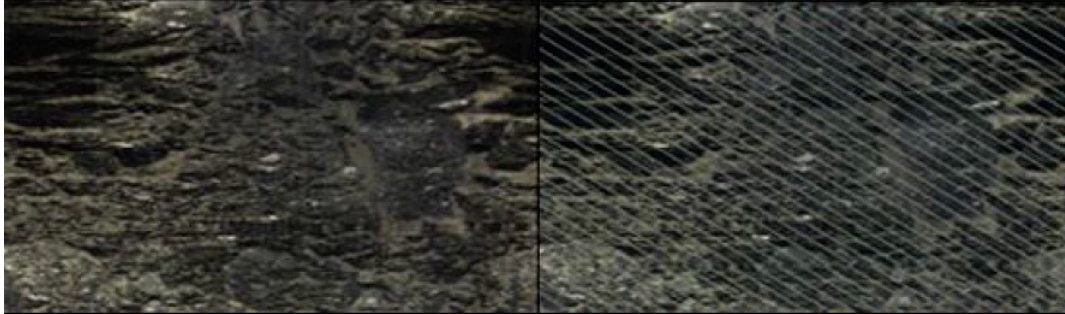


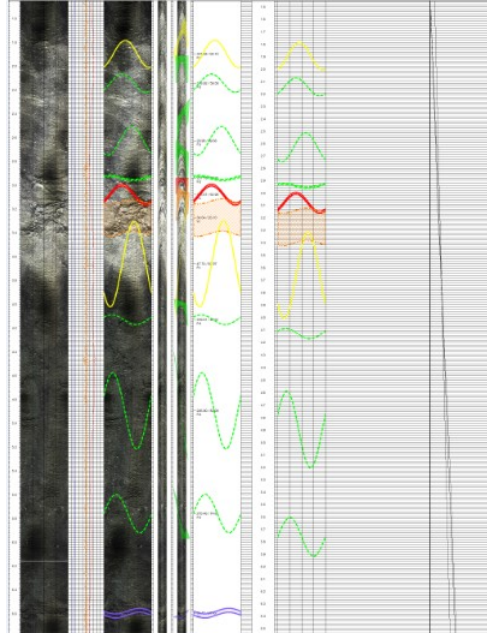
Figure 39: Filing material mapped [8]

The data for each hole was extracted in a .txt file, for the analysis through MATLAB (see Table 4) as example. It includes for each discontinuity, the depth, azimuth, dip and aperture.

Table 4: (Blast N°1, Hole N°3) Extracted data from WellCAD analysis.

Depth (m)	Azimuth (°)	Dip (°)	Aperture (mm)	Discontinuity type
1.45	174.19	15.62	0	Fc
1.61	344.08	30.24	0	Fo
1.74	285.57	36.55	0	Fc
2.01	181.93	62.09	0	Fd
2.78	279.54	61.69	0	Fd
2.81	55.26	22.36	363.41	V
3.08	334.89	26.92	0	Fd
3.44	239.01	64.37	0	Fd
3.7	44.72	15.57	0	Fd
4.18	69.72	23.11	0	Fd
4.34	82.62	57.01	0	Fc
5.35	93.52	10.11	0	Fc
5.91	293.37	73.16	0	Fc
6.79	275.25	16.41	0	Fd
6.86	44.80	9.06	0	Fc
6.98	72.70	16.56	0	Fc
8.56	329.26	51.02	0	Fd
8.8	170.68	53.29	0	Fd
9.76	128.73	30.99	0	Fc

In Table 4 Fc is continuous closed fracture; Fd is discontinuous fracture; Fo is open fracture and V is void.



The mean and standard deviation of the logged length is 22 and 7.4, respectively. A total of 366 fractures have been marked in 17 boreholes drilled in blasts B1 and B5. A summary of the discontinuities considered for the study is shown in Table 5. The statistics of the number of discontinuities marked are also shown in Table 5 for each type. The most frequent discontinuities (sorted in descending order) are Fd, Fc, Fo and V according to the fracture frequency value. The mean 1.9 m-1, the spacing between discontinuities can be qualitatively ranked as moderate [27].

Table 5: Total N° of discontinuities and their frequencies, along with STD and mean values for each hole.

<i>BlastNo./HoleNo.^σ</i>	Fd	Fc	V	Fo	Tot. No. of Fractures	<i>Frequency(m − 1)</i>
B1H1	16	6	2	1	25	2.04
B1H2	22	5	6	2	35	2.80
B1H3	14	7	1	2	24	1.90
B1H4	14	7	1	2	24	1.90
B1H5	6	12	3	1	22	1.80
B1H7	16	11	2	0	29	2.27
B1TV1	12	4	4	2	22	2.10
B1TV2	11	1	0	2	14	1.30
B1TV3	7	5	3	3	18	1.72
B1TV4	3	3	1	1	8	0.90
B1TV5	1	12	2	0	15	1.50
B5H2	15	2	1	2	20	1.50
B5H3	7	1	0	3	11	0.80
B5H4	17	8	0	4	29	2.20
B5H5	17	5	1	10	33	2.50
B5TV1	8	4	2	6	20	2.01
B5TV2	3	5	0	9	17	1.70
Mean	12	5	1	2	22	1.90
<i>STD^σ</i>	5.90	3.40	1.60	2.80	7.40	0.50

- H refers to Blasthole and TV to Televiewer hole

- STD is standard deviation

There are some limitations with the optical televiewer. related with the fact that discontinuities are marked in images, being difficult to know whether they induced a mechanical response while drilling.

4.1.4 Definition of a binary vector for structural characterization

Following the work by A. Fernández [4], a binary sequence (presence/absence) known as D_{obs} has been constructed to correlate discontinuities identified in the borehole walls by the optical televiewer with the response of the drilling rig; in this sequence, ones are assigned to discontinuities and zeros for massive rock (absence of discontinuities) as a function of borehole depth using the same resolution as the measuring while drilling system MWD ,i.e, about 1 cm. To build D_{obs} it is considered that the drill response to a discontinuity is not limited to a single point at a specific depth of the discontinuity, like it is centre (d_{cp}), but rather to the entire intersecting length (d_b) of the discontinuity and the borehole, see Figure 41.

$$d_b = d_{cp} \pm \frac{\phi_h}{2} \cdot \tan \alpha \quad (1)$$

where ϕ_h is the hole diameter and α is the angle of the normal of the discontinuity with the borehole axis. The area of influence of each discontinuity is calculated considering the normal of the discontinuity with the borehole axis [4]. This means that pseudo-vertical discontinuities have a larger influence area than a pseudo-horizontal one. As an example of this approach Figure 42 compare a part of a televiewer log with the resulting binary sequence D_{obs} where zeros representing massive rock are displayed in white and ones representing discontinuities in blue; other fractures than Fc (yellow traces), Fd (green traces), Fo (red traces) and V (grey traces) discontinuity types are discarded for the analysis. The final aim is to calibrate the structural drilling index from the binary sequence D_{obs} .

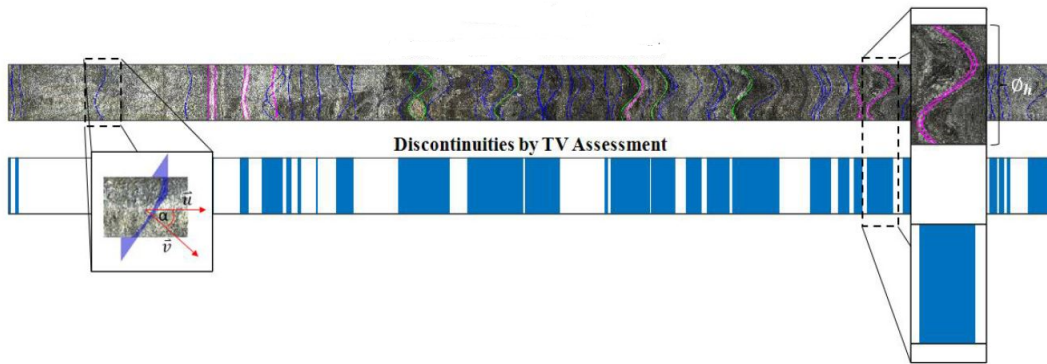


Figure 41: Discontinuities by TV assessment [4]

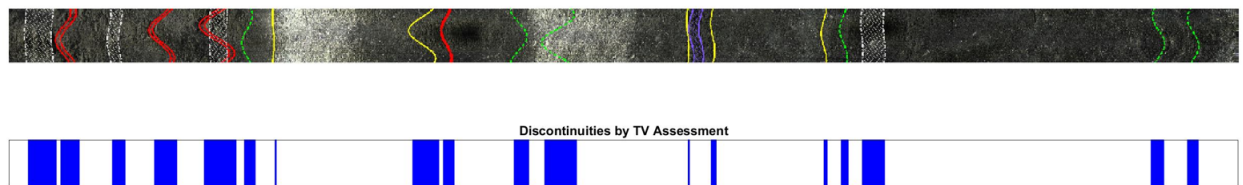


Figure 42: Discontinuity from Optical televiewer assessment (Blast N°1, hole N°9).

4.2 Drilling Characteristics

The drilling machine accessible in El Aljibe is a Tamrock DX-800 from 2008 (see Figure 43), which is equipped with a top hammer rotary-percussive vertical rig, 3.2 m long and 58 cm diameter rods, and a bit with a diameter of 89cm. Due to the fact that the rig does not have a manufactured drilling monitoring system, an in-house MWD system was built as a low-cost and efficient alternative for monitoring the rig's information while drilling (Navarro et al. 2018). Integra automatizacion S.L.U, digitalized the drilling signals via a parallel connection of the already installed sensors for analogical display of the drilling mechanism [28]. The PLC (Programmable Logic Controller) and the HMI (Human Machine Interface) were created to depict live data of pressure and depth parameters in a screen that was mounted in the drill rig. The system converts additionally analogy signals to digital ones for data storage and retrieval.



Figure 43: Tamrock DX-800 top hammer rotary-percussive rig.

A rotary encoder allows to identify an increase in depth during drilling by converting its pulses into linear displacement. The system registers information of drilling parameters at every pulse when the hole depth increases which corresponds to 1cm. Table 6 shows the parameters that the system monitors, along with their units; the drilling time is not monitored, which prevents to calculate the penetration rate.

Table 6: Drilling parameters under study.

Parameter	Code	Unit
Percussive pressure	PP	bar
Feed pressure	FP	bar
Rotation pressure	RP	bar
Damp pressure	DP	bar
Air pressure	AP	bar

The system as well records the hole depth (HD), hole inclination of the mast, the addition of a new rod, and drilling mode (i.e. automatic or manual mode). In order to measure the vertical and horizontal angles of the rods outside the blasthole, two inclinometers were mounted. These values were likewise recorded at a 0.01 m sample interval, in accordance with the monitored parameters.

The electronic sensors used to digitalize the analogic signal of the parameters and the inclination of the mast have the following technical specifications [28]:

- Percussive pressure: a pressure sensor with an output range of 4-20 mA and a pressure range of 0 to 600 bar (maximum pressure 2500) is used. The data is collected using a 15-bit data acquisition card with a resolution of 0.0183 bar.
- Rotation, Feed, and Damp pressures: electronic pressure sensors with a range of 0 to 250 bar (maximum pressure 1200) and an output range of 4-20 mA. The data is collected using a +15 bit data capture card with a resolution of 0.0066 bar.
- Inclinometers: a +15-bit data acquisition card is utilized to collect data with a resolution of 1.9" and maximum measurement angles of $\pm 20^\circ$.
- Air pressure: electronic pressure sensor with a range of 0 to 100 bar.

The logging data is shown on the screen, which is also used to enter the blasthole number and to indicate other parameters like installation of a new rod or a new bit and manual or automatic drilling (see Figure 44).

Additional characteristics of the sensors are the resistance to the vibrations (20 g, 10 to 2000 Hz), response time (1 ms), and working temperature range (-40 to 90 °C).

The following procedures are followed for data logging and storage: the PLC receives electrical signals from pressure, inclination, and depth sensors, which are processed by the program, and they are registered every time the encoder increases a pulse and the following boundary pressure conditions are met [28]:

- The percussive pressure exceeds 80 bar.
- The feed pressure is larger than 30 bar.
- Rotational pressure of at least 25 bar.
- More than 3 bar of air pressure.

After the blast is completely drilled, the data into a text file is copied to a memory card.

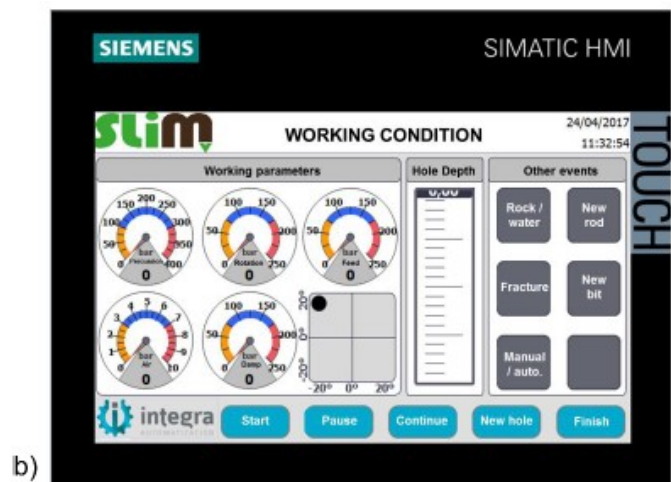


Figure 44: The in-house drill monitoring system installed in the operator-cabin(a), View of the monitoring screen(b) [28]

4.2.1 MWD data processing

MWD parameters response is usually influenced by many factors apart from the rock, for instance the control system elicits variations in the MWD data while the parameters are being adjusted [6]. The hole length affects also to some drilling parameters [20], A series of steps that have been developed throughout the years by many authors [20];[29];[6] to remove the factors that mask the effect of the drilling rig, the flowchart of the signal processing is shown in Figure 45. It includes the following:

- - Filtering the effects due to rod addition.
- - Remove collaring and ending data or the ramp-up operation at the beginning of drilling and systematic drops at the end of the signals that could be as result of the interference of the operator in the drilling process before reaching the final depth of drilling.
- - Remove the dependency of the hole length on drilling parameters [20].

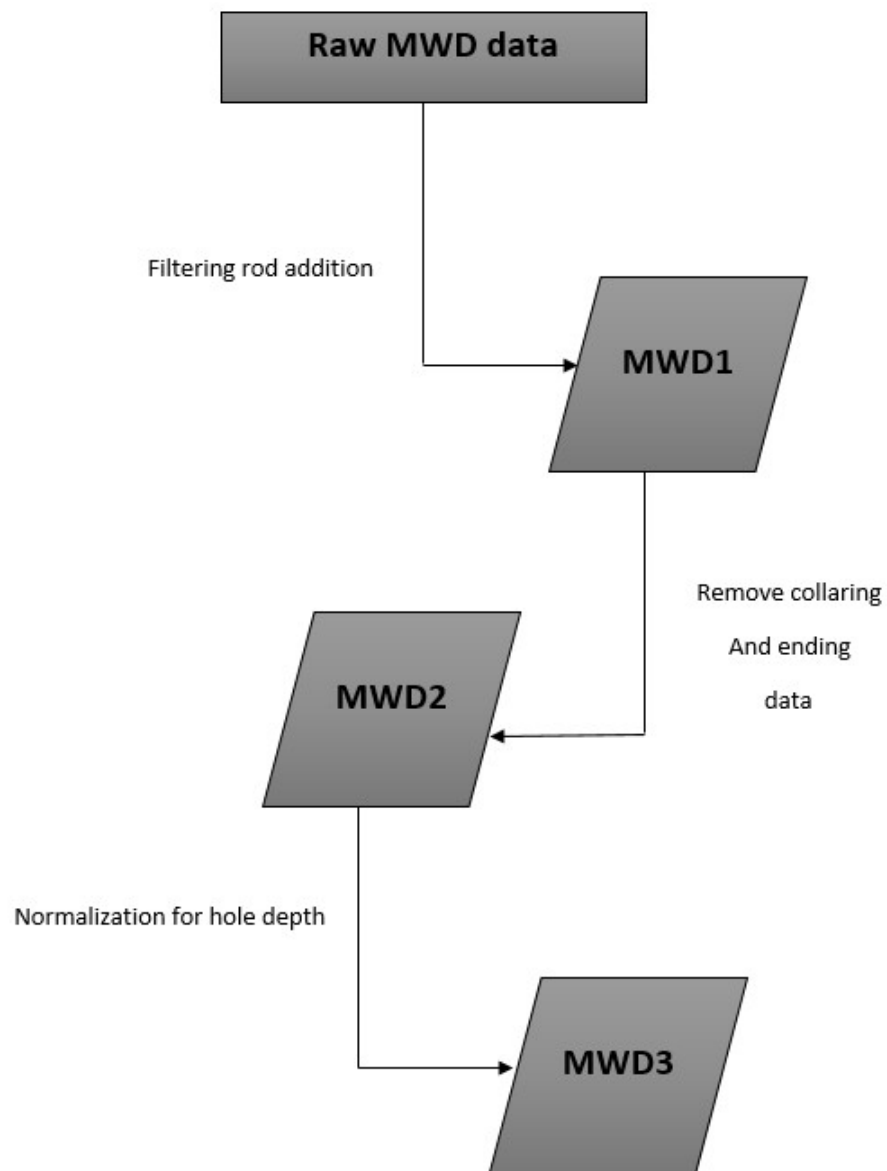


Figure 45: Flowchart showing the MWD data processing steps

The file received from the in-house MWD system, contains nine columns that comprises depth, five pressures, inclination, rod number and drilling mode (auto or manual). The data was organized and processed through Matlab [30]. All unnecessary columns, duplicate and negative values were removed. Figure 46 show an example the parameters recorded in one borehole; values of one indicates manual drilling while zeros show automatic drilling.

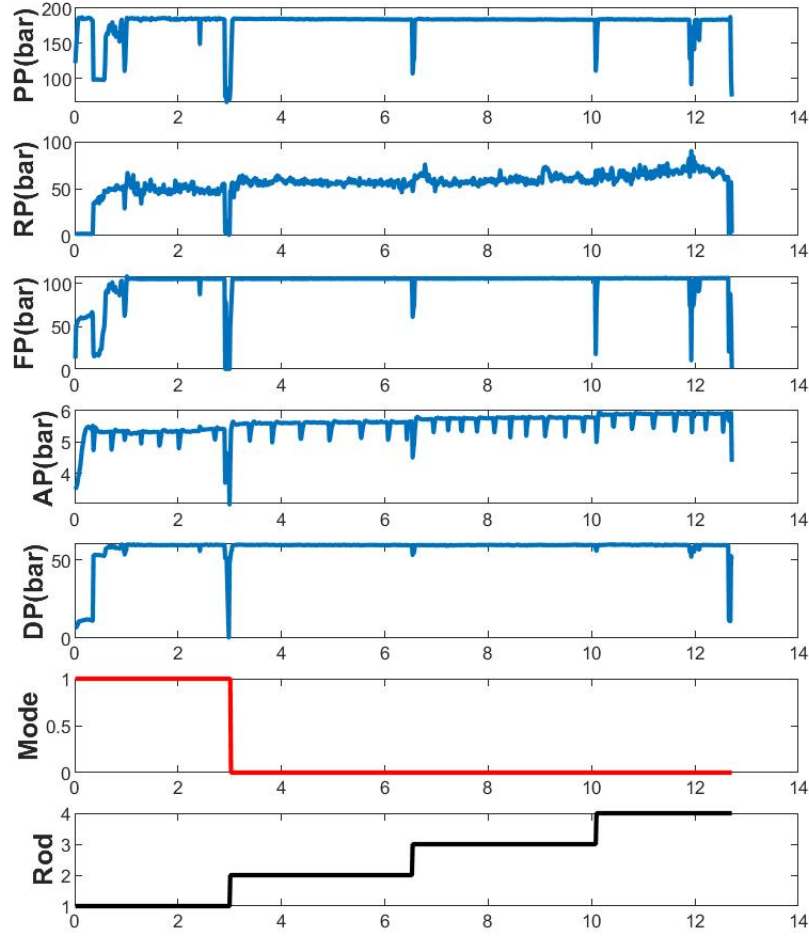


Figure 46: Raw MWD signals (hole No. 1 in blast 1)

Considering that exist two modes of drilling as mentioned before (auto and manual), the auto drilling mode represent 98% of the drilling data, while manual mode is only used in the first part of the hole during the ramp-up mode. To further understand the data, values of the minimum and maximum of each parameter were obtained to know more about the initial ranges of each parameter (see Table 7), moreover, general statistics about the density distribution of all parameters have been calculated and plotted in Figure 47 for each blast with different colours, similar distributions are obtained for RP, AP and DP, while smaller PP and FP are obtained for the blast in blue. The signals for each hole were plotted afterwards against the depth interval for each hole (see Figure 46) to visualize the signals.

Table 7: General statistics about the parameters range, for raw data.

Parameter	Unit	Range	mean	$STD(\sigma)$
Percussive pressure	bar	$17.1 < PP < 190.9$	173.1	5.1
Feed pressure	bar	$0.7 < FP < 171.8$	99.2	2.1
Rotation pressure	bar	$0 < RP < 96.3$	56.1	3
Damp pressure	bar	$0.3 < DP < 60.8$	57.4	0.7
Air pressure	bar	$2.5 < AP < 6.4$	5.5	0.06

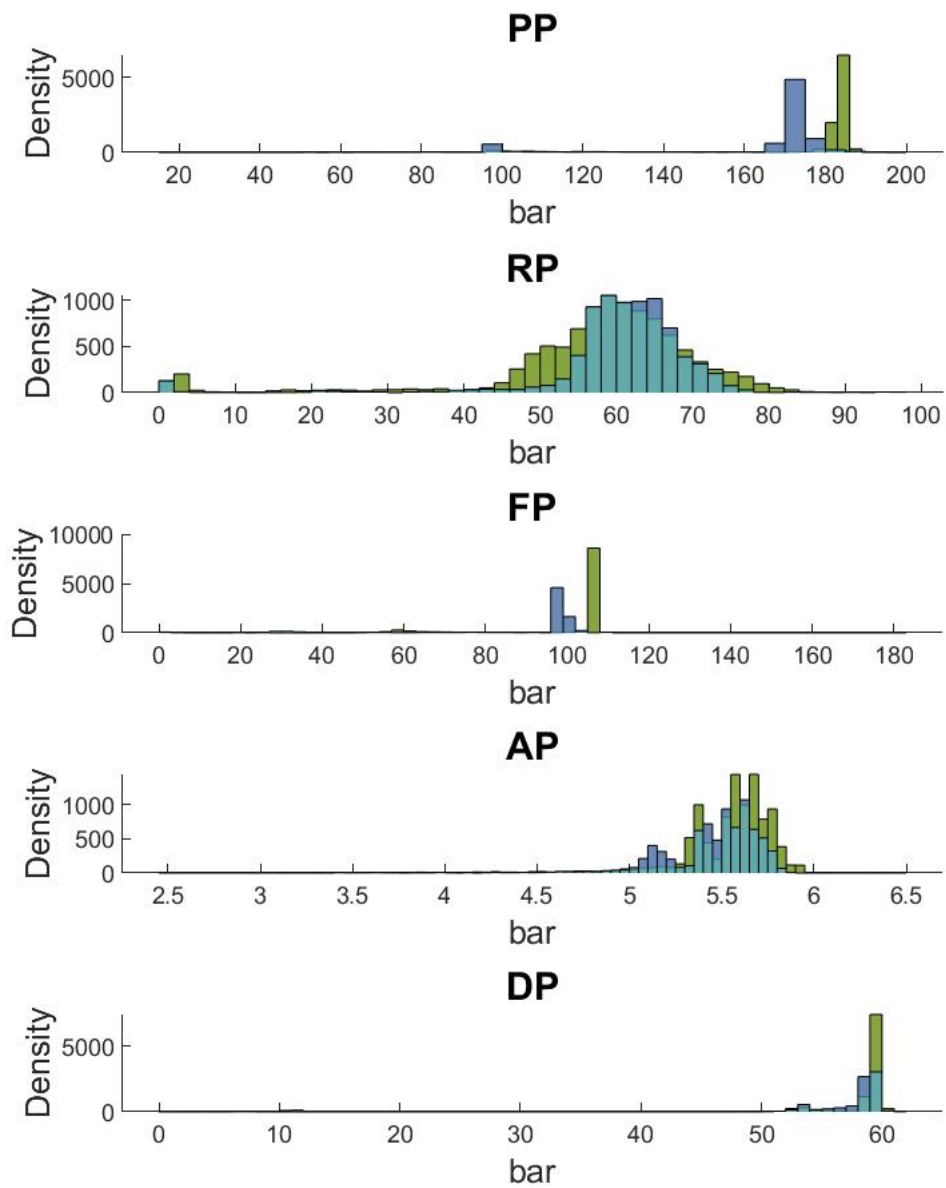


Figure 47: Density distribution of each MWD parameter for each blast. Green bars correspond to blast B1 and blue ones to blast B5.

The different processing stages are explained in detail next:

◆ **Filtering rod addition:**

At the point the drilling matches or reaches the length of the feeder, that corresponds about 3m, a new rod should be inserted to continue drilling. This involves systematic variations of operational parameters when this process of adding a new rod takes place some parameters such as rotation pressure and feed pressure come to a halt and their activity is ceased, at that point the drilling rod is pulled to add the new one at the end of the one that already exists [31].

Figure 48 shows with green rectangles the depth at which a new rod is added, this is clearly shown the drops observed in the bottom graph. This operation produces a clear drop in the PP, FP and DP. In RP the drop occurs only when the second rod is added. These drops are associated with the stop of the system and not related with the response of parameters to the rock mass, hence they must be removed.

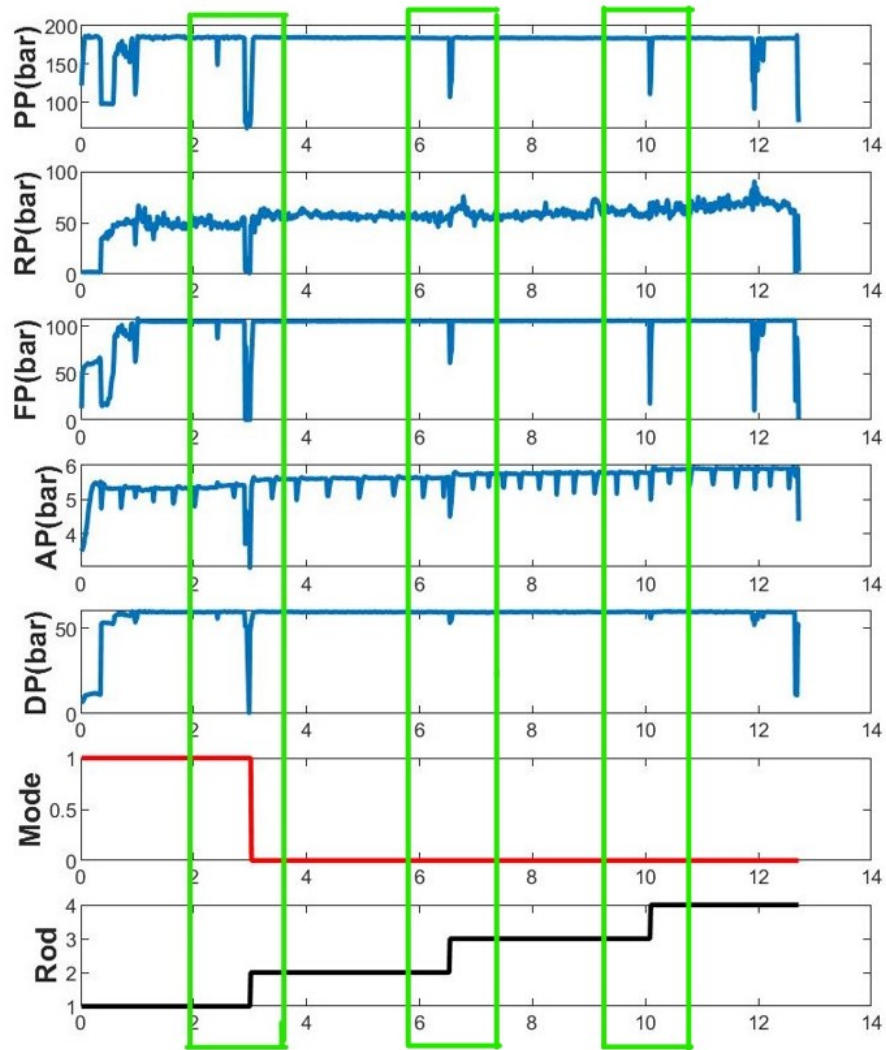


Figure 48: Effect of rod addition (Blast No.1 , hole No.1) marked by a green rectangle.

Processing the data through MATLAB, a moving average with a window of 40 was calculated for all the parameters. From the recorded depth at which every new rod was added, the moving average was applied 10 intervals before and after that depth to obtain the moving average of the signal in that exact position, hence, all systematic drops related to the rod addition were replaced with this average value as is shown in Figure 49, In the figure blue lines represent raw signals and red lines are the new signals after rod addition has been removed.

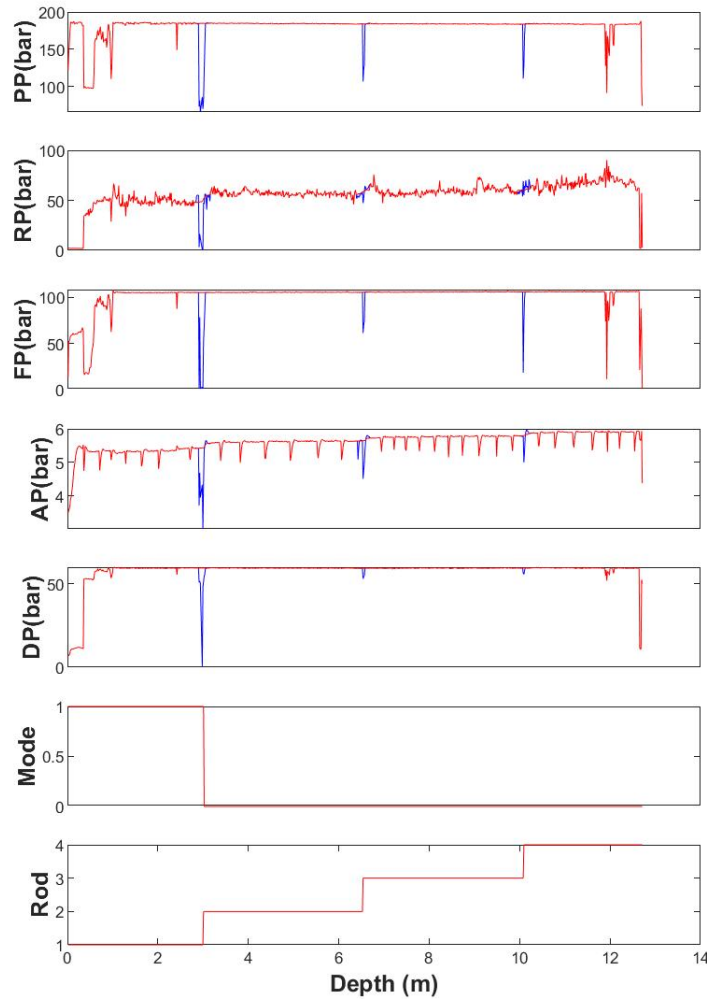


Figure 49: MWD signals before (blue traces) and after (red traces) rod addition removal (Blast N^o1 , hole N^o1)

◆ Removing collaring and ending data:

The ramp-up operation mode, this operation particularly takes place at the beginning of the drilling process when the bit has started penetrating the rock, at this point, low pressures are being applied on the rock to avoid any bending or deviation in the hole and to reach a proper accuracy in the positioning of the boom [31]. This operation happens at range of meters of (0.3-1.5m), hence the values of pressures at that range do not represent the parameters response to the changes in rock properties.

Creating a moving median and using MATLAB based function (`findchangepts`) the position of removing the ramp-up was located for all the holes. Since this depth is smaller than the length of the televiewer logging tool (see Section 4.1), all signals were cut at a depth of 1.47m, as for smaller depths no information on rock discontinuities is obtained.

The presence of a systematic drops between 0.2 and 0.5 m before the bottom of the borehole do not represent the responses of parameters to the rock. Reasons behind such negative values could be either from the intervention of the operator in the drilling process before reaching the final depth or excessive removal of detritus.

An example of the ramp-up mode is shown in Figure 50 with a red rectangle at small depths (0-1.5m) where a strong increase in the signals of all parameters is observed. On the other hand, anomalies at the end of the hole are highlighted with a red rectangle. Those increments and drops in the parameters may be confused with a discontinuity and must be discarded for the analysis, Figure 51 shows the original signal and the part used hereafter.

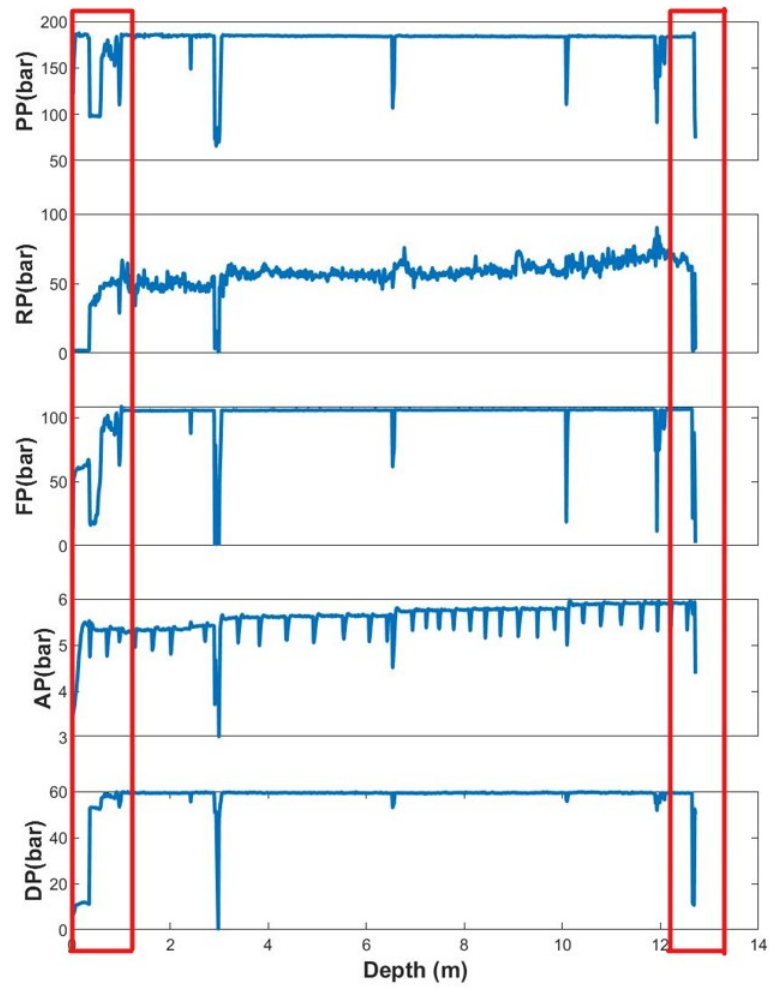


Figure 50: Position of the ramp-up and ending drilling modes in hole No.2 in blast B1.

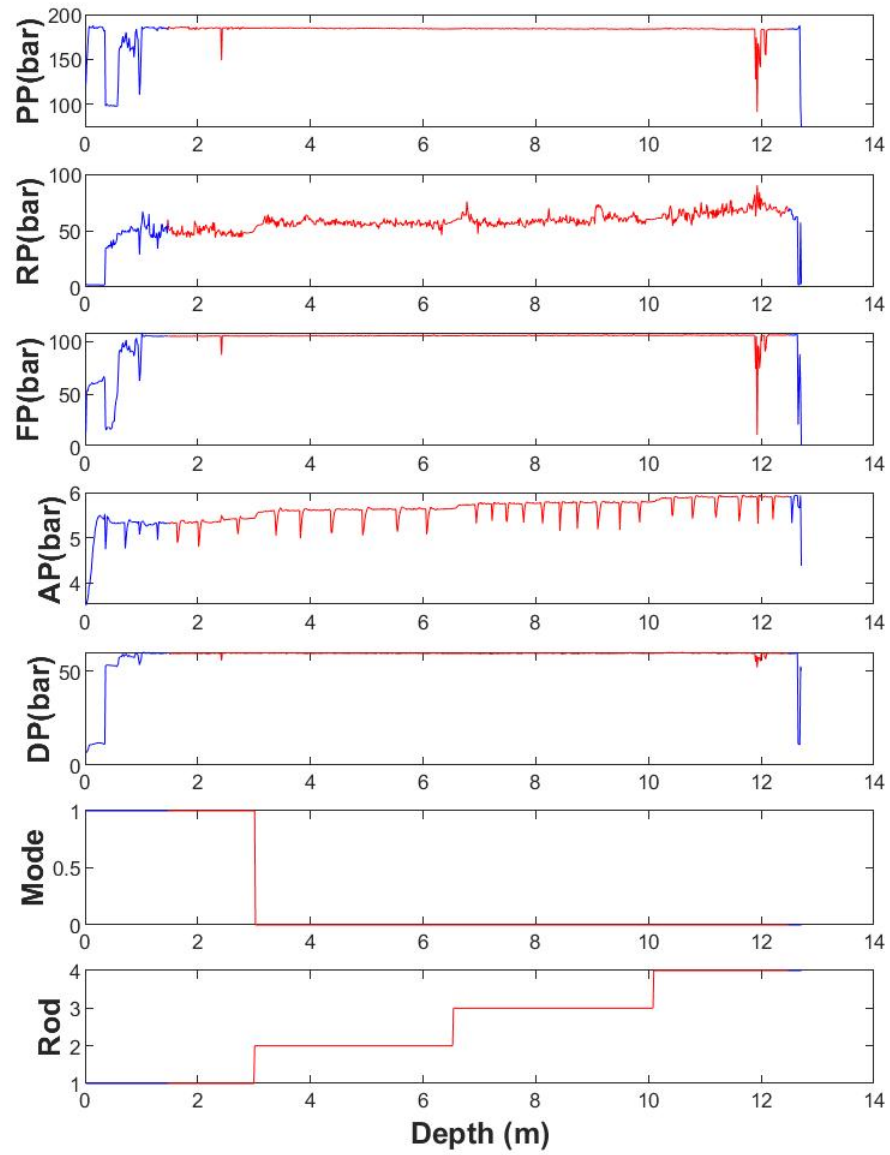


Figure 51: Original signal (blue traces) and signal without collaring and ending effects (red traces) in hole No. 2 in blast B1.

◆ **Normalization for the hole depth:**

The effect of the hole length in drilling parameters is observable in different drilling types, [20] claimed that by averaging the drilling data, we can detect and eliminate these systemic variations. Normally, variations with depth are related to increasing energy losses as holes lengthen due to reduced stress wave energy conveyed along the drill rod, and also by less flushing efficiency with the increase of the hole depth. Moreover, with the increase of the hole depth the resistance resulting from friction between the hole walls and the rod will increase [20].

Despite the fact that all of these factors will have an effect on the overall drilling process, some parameters due to their nature will be more affected, for instance and with reference to the factors mentioned before, the decrease in the energy transmitted along the rod will have more impact on the Feed pressure and the percussive pressure depending on the direction of drilling (horizontal, downwards or upwards) in this study the drilling was downwards, while the decrease in flushing with depth affects directly the air pressure, as for the increment in the frictional resistance with depth, will have repercussions on the rotation pressure and unrealistic values will be recorded that are more representative of this increase in resistance [3].

The correction of the impact of the hole length is done by the following equation:

$$MWD^i c2 = [MWD^i c1 - MWD^i fit, hl] + MWD^1 fit, hl \quad (2)$$

with $i = 1, 2, \dots, L$

Where MWD is a specific MWD signal, i indicates the sample number, L is the total number of these logs, $MWD^i c1$ is a polynomial of degree 3 to 5 fitted to average MWD signal of each hole and i . $MWD^1 fit, hl$ is the value of the polynomial at depth zero [6].

To investigate whether drilling parameters are affected by the hole depth, the average signal for all the holes is calculated. At first the minimum and maximum values of hole depth for the entire data are calculated (1.47m) and (14.40m) respectively, from these two measurements a vector was created that represents a hole length every 0.1 m in the range of the minimum

and maximum values obtained. This vector was used to interpolate the data of each hole and eventually obtain the mean drilling parameters for the holes monitored, (see Figure 52). The figure shows that the rotation pressure (RP) and air pressure (AP), (blue and green signals respectively) increase with the borehole length while the percussive (PP) and feed pressure (FP) show no systematic effect, As drilling is downward the hole length has no greater effect on those two parameters in this case.

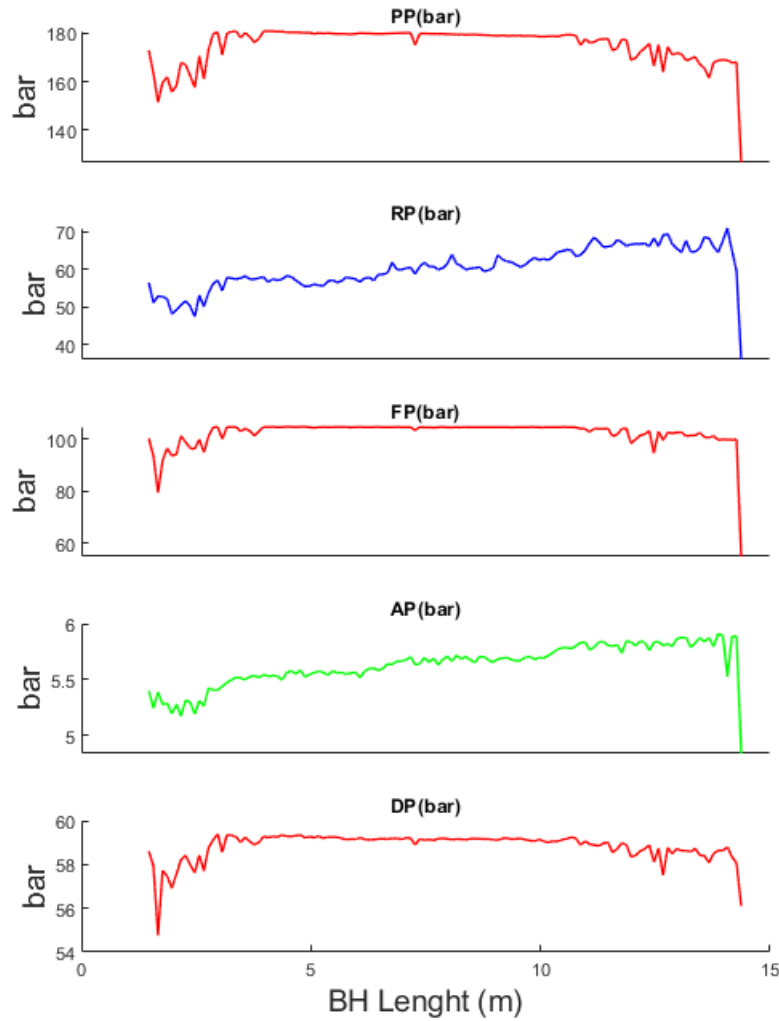


Figure 52: Average signal of each MWD parameter.

To apply (Eq.1) with MATLAB instruction (polyfit) a polynomial curve fitting with degree 5 was done for the average values and the Y-intercept calculated; this is only applied for (RP) and (AP) signals. The average corrected signal is shown in Figure 53.

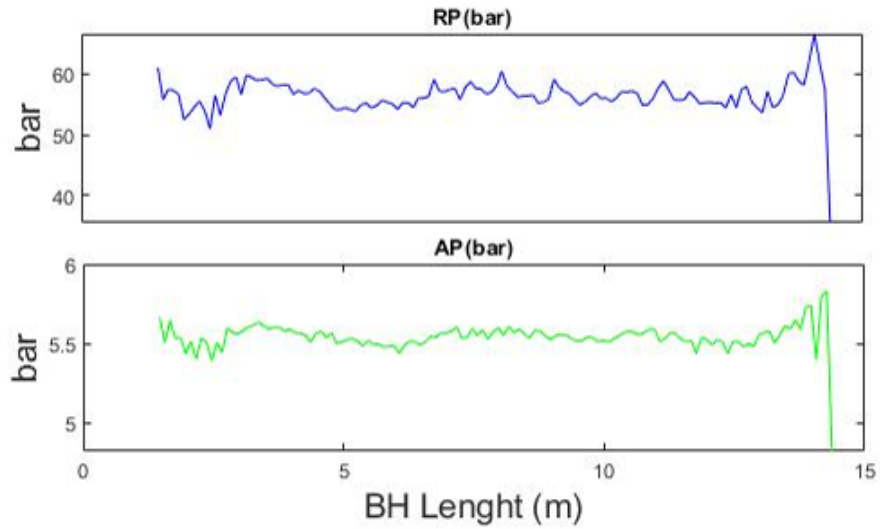


Figure 53: Average corrected signal for RP and AP parameters.

The normalization of hole depth for each hole was plotted afterwards against the previous signal before normalization for RP and AP signals, looking at Figure 54 where red lines represents the normalized signals and blue signals before normalization we can see the variation between the two signals and the effect of the hole dependency on the drilling parameters. No normalization is carried out for PP, FP and DP.

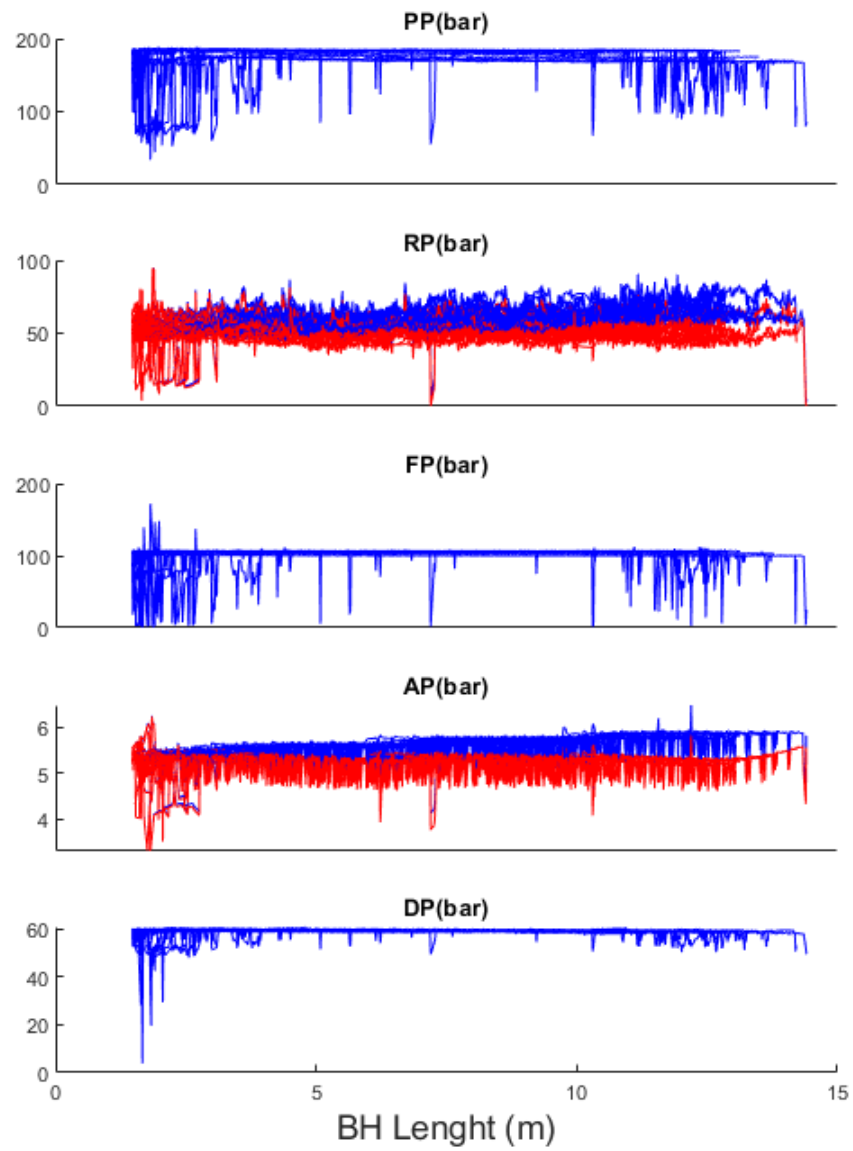


Figure 54: Non normalized (blue traces) and normalized MWD signals (red traces) for the hole depth for all boreholes.

4.2.2 Discontinuity index DI

Once the data of MWD has been processed and filtered now we can obtain the Discontinuity index (DI) for the analysis. This is calculated based on the variations in the recorded parameters [2] as variations in some drilling parameters happens in the presence of discontinuity [20]. This is the case of rotation pressure (RP) and penetration rate (PR) that in the presence of a discontinuity, shows noticeable oscillations [32]. All these variations are pointed out and calculated as the sum of the residuals over a defined interval along the borehole. For example, authors such as [2] and [3] have combined those variations into a discontinuity index DI. The most recent DI proposed by [3] is built as follows:

$$DI_i = \sqrt{0.5\left(\frac{PR_{var,i} - PR_{var}}{stdPR_{var}}\right)^2 + 0.5\left(\frac{RP_{var,i} - RP_{var}}{stdRP_{var}}\right)^2} \quad (3)$$

with $i=1,2,...,L$

Where:

- $PR_{var,i}$ and $RP_{var,i}$ are variability of the penetration rate and rotation pressure calculated as a moving variance at each sample point i .

- L is the number of points.

- PR_{var} and RP_{var} are the mean of the variability of PR and RP, respectively.

- $std(PR_{var})$ and $std(RP_{var})$ are the standard deviation of PR and RP.

To improve the recognition ability of discontinuities, a modification of (Eq.2) has been proposed in which the combination of the parameters along with their weights are taken into account to try to find which combination of parameters is the best option for a particular operational situation [4].

$$DI_i = \sqrt{\sum_{j=1}^n \beta_j \left(\frac{vari(MWD_j) - var \overline{MWD_j}}{std(var MWD_j)} \right)^2} \quad (4)$$

with $i=1,2,\dots, L$

Where n is the number of MWD parameters considered, L is the number of records for each borehole and $vari(MWD_j)$ is the moving variance at the sample point i calculated through a sliding window of the j^{th} MWD parameter (this is done through the MATLAB function, `movvar` with a length of 14 sample or 14 mm); $std(var MWD_j)$ and $var \overline{MWD_j}$ are the standard deviation and mean of the moving variance for the j^{th} MWD parameter respectively; β_j is the weight of the j^{th} MWD parameter, so $\sum_{j=1}^n \beta_j = 1$.

For a given combination of drilling parameters and weights, a binary sequence is built. In this sequence, ones (that correspond to discontinuities) are assigned at depths in which the peaks of the DI signal exceed a threshold value. In other words, the presence of discontinuities could be linked to the key peaks in the DI signals.

Several Discontinuity indexes from on different combinations of two, three and four parameters of the parameters under study (PP, RP, FP, AP and DP) with different weights in (Eq.3) are built. For each of these discontinuity indexes, 10 binary sequences are calculated using a different threshold value that is obtained as the percentile 50, 55, 60, . . . or 95.

To determine the combination of MWD parameters and weights, as well as the threshold percentile , which leads to the best identification of the discontinuities in the borehole, the binary sequences from the DI (D_{DI}) are compared with the corresponding sequence D_{obs} (see Section 4.1.4) from televiewer images of that hole metrics for binary classifiers are used.

To account for errors in the exact position of discontinuities and the fact that the drill rig is influenced by conditions at prior depths, a cross correlation analysis with an offset lag of 10 between D_{DI} and D_{obs} has been carried out. , This allows to obtain the relative position between D_{DI} and D_{obs} at which the correlation is maximum. For this relative position, the classification accuracy or fraction of massive rock and discontinuities that are correctly classified is calculated [33].

$$Acc = \frac{(TP + TN)}{(P + N)} \quad (5)$$

Where TP and TN are True Positives (i.e., number of samples of discontinuities correctly predicted), and True Negatives (i.e., number of samples of massive rock correctly predicted), respectively; and P and N are the number of samples of discontinuities and massive rock, respectively in D_{obs} .

5 Results

Table (8) and (9) show the classification accuracy for discontinuity indexes based on two parameters and three parameters, respectively; data is sorted in descending order of the mean classification accuracy for all the boreholes. For all the combinations shown the best results are obtained using a threshold of 95%.

For two parameters combination, (see Table 8), the accuracy ranges between 69.1% to 70.7%. The highest identification is obtained by combining Percussive pressure (PP) and air pressure (AP), with each parameter weighted 20% and 80%, respectively lead to a mean accuracy of, 70.7%. Generally, the best results are obtained when air pressure (AP) is considered as can be seen from Table 8, involving slightly smaller accuracies down to 70.4%. In these combinations (AP) has the highest weight compared to the other. This could be explained as result of the decreasing of flushing efficiency with increase of depth and not related to the parameter interaction with the rock mass conditions.

Combinations of three parameters involve a slightly worst performance , (see Table 9). In the best case, accuracies are 69.7%. This occurs for the combination of percussive pressure (PP), feed pressure (FP) and damp pressure (DP) with weights of 20%, 70% and 10%, respectively. Accuracies about 70% are obtained when the (AP) is included in the DI. For other parameters involved, the accuracy decreases but it is still near a 70%.

Table 8: Performance of the discontinuity index formed by two parameters; a threshold percentile of 95 is obtained to build D_{DI} .

Parameters	Weights($\beta\%$)	Similarity index, Acc (%)	Std. classification Acc. (%)
'PP/AP'	20-80	70.7	0.09
'FP/AP'	30-70	70.7	0.09
'AP/DP'	70-30	70.6	0.09
'RP/AP'	10-90	70.4	0.09
'FP/DP'	10-90	69.7	0.1
'PP/FP'	50-50	69.6	0.1
'PP/DP'	20-80	69.5	0.1
'RP/DP'	20-80	69.4	0.1
'RP/FP'	10-90	69.2	0.1
'PP/RP'	40-60	69.1	0.1

Table 9: Performance of the discontinuity index formed by three parameters; a threshold percentile of 95 is obtained to build D_{DI} .

Parameters	Weights($\beta\%$)	Similarity index, Acc (%)	Std. classification Acc. (%)
'PP/FP/DP'	20-70-10	69.7	0.1
'RP/AP/DP'	80-10-10	69.6	0.1
'FP/AP/DP'	80-10-10	69.6	0.1
'PP/AP/DP'	80-10-10	69.6	0.1
'PP/FP/AP'	20-70-10	69.4	0.1
'PP/RP/FP'	30-50-20	69.4	0.1
'RP/FP/DP'	10-80-10	69.3	0.1
'PP/RP/DP'	20-30-50	69.3	0.1
'PP/RP/AP'	30-50-20	69.2	0.1
'RP/FP/AP'	20-70-10	69	0.1

To demonstrate the recognition performance of the DI marked in bold in Table 8. Figure 55 and Figure 56 compare the televiewer log (top) and the binary sequences, D_{obs} (central) and D_{DI} (bottom) for the holes with best and worst classification accuracy. These are blasthole No 2 and televiewer No.3 in blast B1, for which the classification accuracy is 55% and 86%, respectively. To further explain, in Figure 55 just about six discontinuities are correctly predicted (TP) that is about 20% of the total number of discontinuities in that particular blasthole, while 91% of massive rock is correctly predicted (TN). On the contrary, for Figure 56 a zero correct prediction of discontinuities (TP) took place and 97% of massive rock is correctly predicted (TN). This explains the classification accuracies for the two blastholes.

The yellow rectangles in Figure 55 show the recognition of the different types of discontinuity, the mismatching of the fractures being identified between D_{obs} and D_{DI} are caused by discrepancies in the calculated discontinuity extension and the response in drill parameters. It appears that the D_{DI} does not provide so wide fracture zones as observed in D_{obs} . This result could be an indication that the influence of inclined fractures in the response of the drill rig is smaller than it is considered to compute D_{obs} (see Section 4.1.4). It can be seen in Figure 55 that there are three false positive in D_{DI} (i.e. areas of massive rock that are incorrectly classified as discontinuities in D_{DI}). In this regard, using a lower threshold increases the number of false positives. The massive rock (white zones) can be seen that they are generally identified by the drilling response. Figure 56 shows that none of the fractures observed in the borehole are identified by drilling data, that provides in addition a false positive that matches an area in which a change of the color is observed in televiewer log.

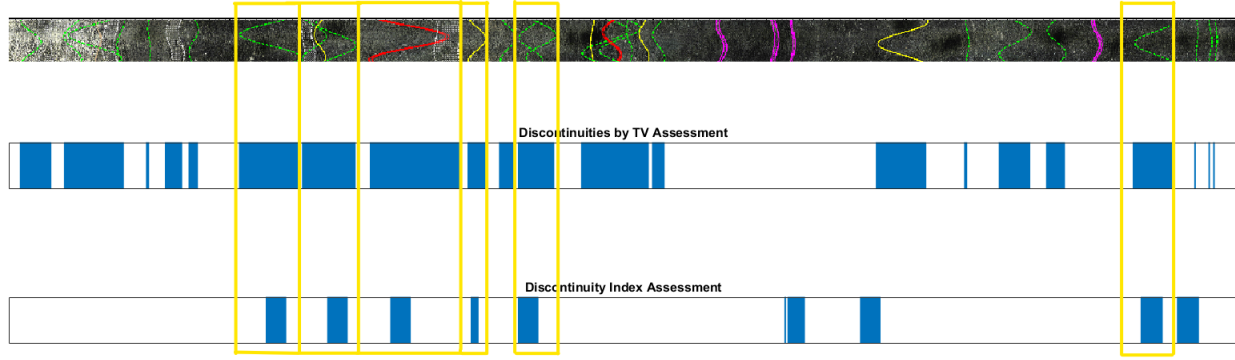


Figure 55: Televviewer log, and binary sequences (D_{obs} & D_{DI}) and for blasthole No. 2 in blast B1; .only Fc (yellow traces), Fd (green traces), Fo (red traces) and V (grey traces) discontinuity types are considered.

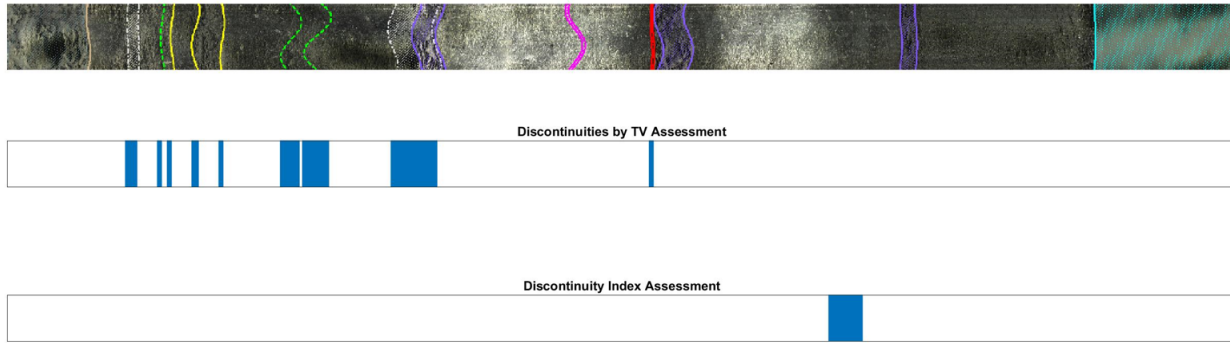


Figure 56: (Televviewer log, and binary sequences (D_{obs} & D_{DI}) for televviewer 3 in blast B1 ; only Fc (yellow traces), Fd (green traces), Fo (red traces) and V (grey traces) discontinuity types are considered.

Table 10 compares the fractures (or number of ones) from the binary sequence D_{obs} obtained with televviewer with respect to the fractures from the drilling data in D_{DI} . The percentage of samples recognized as fractures (or true positives) by the DI is around a 10% for Fd, Fc and Fo, while for voids is slightly larger and near 15%. These fractures present a larger aperture than the rest of the other fractures and it can better detected. The low percentages for discontinuities are an indication that:

- Not all the fracture zone is identified, which suggests that the procedure to calculate D_{obs} must be reviewed and that the area of influence of inclined fractures must be reduced.
- Not all the fractures produce a variability in MWD signals. It must be then investigated

whether they produce a change in the pressure signal (i.e. higher or lower FP for instance). This is considered by other works [3] that use a linear combination of the pressures (FP, DP, AP, PP) and the DI to detect discontinuities. Table 10 shows that the recognition capacity of massive rock is good.

Table 10: Recognition capacity of the DI marked in bold in (Table.8) for each discontinuity type.

Type of discontinuity	Fractures in D_{obs}	Fractures in D_{DI}	DI/Dobs(%)
Discontinuous (Fd)	1870	184	9.8
Continuous (Fc)	911	89	9.7
Voids (V)	364	52	14.2
Open (Fo)	695	69	9.9
Massive rock (MR)	8100	7513	92.7

6 Conclusion

This work shows a procedure to detect discontinuities based on the noise caused in the performance of the drilling rig. For this, measurements from 17 boreholes in two blasts at an aggregate quarry have been used. The boreholes were mainly drilled in automatic mode with a top-hammer rotary percussive rig equipped with an in-house system that monitors the rig performance, namely: percussive, rotation, feed, air and damp pressures. The rock condition has been quantified from televiewer logs analysed in WellCAD to map discontinuities and assess their direction and aperture. From these data, a binary sequence indicating presence / absence has been built considering that the area of influence of each discontinuity increases as it is more inclined with respect to the borehole axis.

Drilling data has been processed to remove spurious factors caused by rod addition, collaring-ending drilling modes, and the influence of the hole depth using state of the art techniques. The moving variance of each processed drilling signal has been used to build several discontinuity indexes. These comprise all available combinations of two, and three normalized moving variances of drilling data with different weights. For each of these indexes, several thresholds from 95 to 50 are considered to build the corresponding binary sequence from drilling data. This involves that one's (or discontinuities) are assigned at depths in which the peaks of the DI signal exceed the threshold value.

To define the best combination of drilling parameters, weights and threshold percentile, the classification accuracy between the binary sequence from televiewer and MWD is used. This is maximum, near 71% for a combination of the percussive and air pressure with weights of 20 and 80%, respectively and threshold percentile of 95%. Similar results are obtained with the other combinations of two parameters in which the pressure of the flushing fluid is considered. Combinations of three parameters provide slightly worst results.

For the DI and the associated binary sequence that provides the best results, it is observed that 93% of the samples of massive rock are well predicted, while the performance for discontinuities is down to 14% in the best case. The reasons for these results, that must be investigated

in the near future, are:

- The effect of inclined fractures in the drill response is probably smaller than it is assumed in the binary sequence obtained from televiewer data.

- Not all the fractures produce a significant variability in drilling data and therefore to increase the recognition ability, some other drilling parameter must be also considered. This involves, a linear combination of the pressures recorded and the discontinuity index.

- Not all discontinuities marked in the televiewer logs have an effect in the rig performance and it is necessary a better understanding of discontinuities characteristics that have a major effect in the response of the drill rig.

7 References

- [1] SLIM, “Sustainable low impact mining,” *SLIMJ PROJECT*, 2017. [Online]. Available: <https://cordis.europa.eu/project/id/730294>.
- [2] R. Ghosh, “Assessment of rock mass quality and its effects on charge ability using drill monitoring technique,” Ph.D. dissertation, Luleå tekniska universitet, 2017.
- [3] T. Navarro, P. Hartlieb, J. A. Sanchidrián, *et al.*, “Blastability and ore grade assessment from drill monitoring for open pit applications,” *Rock Mechanics and Rock Engineering*, vol. 54, no. 6, pp. 3209–3228, 2021.
- [4] A. Fernández, J. A. Sanchidrián, P. Segarra, *et al.*, “Advances on rock structural recognition from drill monitoring in underground mining.(submitted),” *Tunneling and Underground Space Technology*, 2022.
- [5] MATLAB, *version 7.10.0 (R2021a)*. Natick, Massachusetts: The MathWorks Inc., 2021.
- [6] Navarro, “The use of measure while drilling for rock mass characterization and damage assessment in blasting,” Ph.D. dissertation, ETSI_Energia, 2018.
- [7] M. Bernardini, “Application of lidar and photogrammetry methods at el aljibe quarry (toledo, spain) to characterize the rock mass for fragmentation prediction in rock blasting through kuz-ram and xp-frag models,” Ph.D. dissertation, Politecnico di Torino, 2019.
- [8] C. Marilena, M. Bernardini, and S. Zocca, “Application of in-hole camera and photogrammetry to create calibrated discrete fracture networks and obtain the in-situ block size distribution of a rock mass to blast,” 2021.
- [9] J. L. Hernández Enrile, “Evolución microestructural de rocas cuarzo-feldespáticas como resultado del aumento de la deformación en la milonita de toledo.,” 1981.
- [10] S. Gómez, J. A. Sanchidrián, and P. Segarra, “Near-field vibration from blasting and rock damage prediction with a full-field solution,” *International Journal of Rock Mechanics and Mining Sciences*, vol. 134, p. 104357, 2020.
- [11] J. Imber, R. Holdsworth, S. Smith, S. Jefferies, and C. Collettini, “Frictional-viscous flow, seismicity and the geology of weak faults: A review and future directions,” *Geological Society, London, Special Publications*, vol. 299, no. 1, pp. 151–173, 2008.
- [12] M. G. IGME, “Instituto geológico y minero de españa,” *Madrid, Spain*, pp. 569–572, 2018.
- [13] S. Slob, “Automated rock mass characterisation using 3-d terrestrial laser scanning,” 2010.

- [14] C. Torres, “Geometric characterization of rock mass discontinuities using terrestrial laser scanner and ground penetrating radar,” *Enschede, Netherlands: International Institute for Geo-information Science and Earth Observation*, 2008.
- [15] C. Cunningham, “The kuz-ram fragmentation model—four years on,” in *Brighton conference proceedings*, Society of Experimental Mechanics, Bethel, vol. 1987, 1987, pp. 457–487.
- [16] —, “The kuz-ram fragmentation model—20 years on,” in *Brighton conference proceedings*, European Federation of Explosives Engineers, Kolmården, Sweden, vol. 2005, 2005, pp. 201–210.
- [17] J. A. Sanchidrián and F. Ouchterlony, “A distribution-free description of fragmentation by blasting based on dimensional analysis,” *Rock Mechanics and Rock Engineering*, vol. 50, no. 4, pp. 781–806, 2017.
- [18] H. Schunnesson, “Drill process monitoring in percussive drilling for location of structural features, lithological boundaries and rock properties, and for drill productivity evaluation,” Ph.D. dissertation, Luleå tekniska universitet, 1997.
- [19] J. P. Peck, “Performance monitoring of rotary blasthole drills,” 1989.
- [20] H. Schunnesson, “Rock characterisation using percussive drilling,” *International journal of rock mechanics and mining sciences*, vol. 35, no. 6, pp. 711–725, 1998.
- [21] W. Hustrulid, “Method selection for large-scale underground mining,” *Proceedings of MassMin*, pp. 29–56, 1971.
- [22] Pearse, “Hydraulic rock drills,” *Mining, Magazine*, 1985.
- [23] ALT, *Userguide:ql40 obi-2g optical*, Advanced Logic Technology sa, Denver Colorado. U. S. A., Apr. 2012. [Online]. Available: <https://mountsopris.com/ql40-obi-2g-optical-televiewer/>.
- [24] T. Gomes, P. Segarra, A. Pérez Fortes, and G. Xisheng, “Procedure for rock mass characterization with photogrammetry,” SLIM Technical Report, Tech. Rep., 2017.
- [25] S. Li, X.-T. Feng, C. Wang, and J. Hudson, “Isrm suggested method for rock fractures observations using a borehole digital optical televiewer,” *Rock mechanics and rock engineering*, vol. 46, no. 3, pp. 635–644, 2013.
- [26] —, “Isrm suggested method for rock fractures observations using a borehole digital optical televiewer,” in *The ISRM Suggested Methods for Rock Characterization, Testing and Monitoring: 2007-2014*, Springer, 2012, pp. 159–168.

- [27] N. Barton *et al.*, “Suggested methods for the quantitative description of discontinuities in rock masses,” *ISRM, International Journal of Rock Mechanics and Mining Sciences & Geomechanics Abstracts*, vol. 15, no. 6, pp. 319–368, 1978.
- [28] J. Navarro, P. Segarra, J. Sanchidrián, *et al.*, “Application of an in-house mwd system for quarry blasting,” in *Proceedings of the 12th international symposium on rock fragmentation by blasting, Fragblast*, vol. 12, 2018, pp. 203–207.
- [29] R. Ghosh, H. Schunnesson, and U. Kumar, “The use of specific energy in rotary drilling: The effect of operational parameters,” in *International Symposium on the Application of Computers and Operations Research in the Mineral Industry: 23/05/2015-27/05/2015*, 2015.
- [30] MATLAB, *Matlab — Wikipedia, the free encyclopedia*, [Online; accessed 1-June-2022], 2022. [Online]. Available: <https://en.wikipedia.org/w/index.php?title=MATLAB&oldid=1090198052>.
- [31] J. Navarro, H. Schunnesson, R. Ghosh, P. Segarra, D. Johansson, and J. Á. Sanchidrián, “Application of drill-monitoring for chargeability assessment in sublevel caving,” *International journal of rock mechanics and mining sciences*, vol. 119, pp. 180–192, 2019.
- [32] R. Ghosh, A. Gustafson, and H. Schunnesson, “Development of a geological model for chargeability assessment of borehole using drill monitoring technique,” *International Journal of Rock Mechanics and Mining Sciences*, vol. 109, pp. 9–18, 2018.
- [33] R. R. Sokal, “A statistical method for evaluating systematic relationships,” *Univ. Kansas, Sci. Bull.*, vol. 38, pp. 1409–1438, 1958.